*Reviews in Economic Geology*, v. 18, pp. 339–365

# Chapter 14

# Lithium Brines: A Global Perspective

Lee Ann Munk,[1,†] Scott A. Hynek,[2] Dwight C. Bradley,[3,*] David Boutt,[4] Keith Labay,[3] and Hillary Jochens[1]

[1] *Department of Geological Sciences, University of Alaska Anchorage, 3101 Science Cir., Anchorage, Alaska 99508*

[2] *Earth and Environmental Systems Institute and Department of Geosciences, Pennsylvania State University, 302 Hosler, University Park, Pennsylvania 16802*

[3] *U.S. Geological Survey, 4210 University Drive, Anchorage, Alaska 99508*

[4] *Department of Geosciences, University of Massachusetts Amherst, 611 N. Pleasant St., 248 Morrill IV South, Amherst, Massachusetts 01002*

**Abstract**

Lithium is a critical and technologically important element that has widespread use, particularly in batteries for hybrid cars and portable electronic devices. Global demand for lithium has been on the rise since the mid-1900s and is projected to continue to increase. Lithium is found in three main deposit types: (1) pegmatites, (2) continental brines, and (3) hydrothermally altered clays. Continental brines provide approximately three-fourths of the world's Li production due to their relatively low production cost. The Li-rich brine systems addressed here share six common characteristics that provide clues to deposit genesis while also serving as exploration guidelines. These are as follows: (1) arid climate; (2) closed basin containing a salar (salt crust), a salt lake, or both; (3) associated igneous and/or geothermal activity; (4) tectonically driven subsidence; (5) suitable lithium sources; and (6) sufficient time to concentrate brine. Two detailed case studies of Li-rich brines are presented; one on the longest produced lithium brine at Clayton Valley, Nevada, and the other on the world's largest producing lithium brine at the Salar de Atacama, Chile.

## Introduction

Lithium is a critical and technologically important element used in ceramics, glass, lubricants, light-weight alloys, medicine, and batteries. The use of Li ion batteries in electric cars and electronic devices has increased the global demand for lithium, a trend that is likely to continue. Lithium-rich brines are the most economically recoverable Li source on the planet. Therefore, it is important to understand the genesis of these deposits in order to develop exploration models for continued discovery of new deposits.

Lithium is found in three main types of deposits: (1) pegmatites, (2) continental brines, and (3) hydrothermally altered clays. Lithium is a lithophile element because it has a low density of 0.53 g/cm$^3$, an ionic charge of +1, and an ionic radius of 0.79. For comparison $Na^+$ has an ionic charge of +1 but a larger ionic radius of 0.99, and $Mg^{2+}$ has an ionic charge of +2 and an ionic radius of 0.72. The lithophilic characteristics of Li and the fact that it is a trace element explain why it concentrates in the late phases of both hydrothermal and low-temperature fluids. This generally explains its association and geochemical behavior in the three deposit types. In particular, for continental brines there is evidence that both evaporative concentration and hydrothermal inputs have a significant impact on concentrating Li in brines. These concentrating processes are effective for Li because it is relatively incompatible and geochemically conservative, both in magmatic systems and low-temperature solutions. From a Li brine production standpoint the Mg/Li ratio of the starting and final processed brines is important because Mg causes chemical interferences in the brine purification process. Ultimately, the initial brine composition determines the production process.

Lithium-rich brine deposits account for about three-fourths of the world's lithium production (U.S. Geological Survey, 2011). These Li-rich continental (nonmarine) brines are the focus of this paper. Economically viable Li-rich brines contain varying amounts of the major cations and anions (Na, K, Mg, Ca, Cl, $SO_4$, and $CO_3$), which can form a range of ionic salts (Warren, 2010). The composition of the source rocks, inflow waters, and the resulting brine composition dictate how the brine will evolve once it undergoes evaporation and mineral precipitation (Eugster, 1980). These brines can also contain appreciable Li, B, Ba, Sr, Br, I, and F, and in the case where Li is concentrated on the order of 100s of mg/L these deposits can be classified as having potential economic viability with respect to Li extraction.

It is known that Li can also accumulate in deep oilfield brines, such as those associated with the Smackover Formation in the Gulf Coast of the United States (Collins, 1976) or the Devonian strata of the Appalachian Plateau of Pennsylvania (Dresel and Rose, 2010). Some brines are reported to contain 100s of mg/L but typically they have low concentrations of Li and are usually greater than 1 km deep, preventing development (Gruber et al., 2011). There are also occurrences of closed basins with abundant saline ground and surface waters which are not enriched in Li. One example is the ephemeral lakes of southwestern Australia, many of which may have occupied closed basins since the Eocene and are hosted by diverse and highly weathered igneous and metamorphic rocks of the Archean Yilgarn craton (Benison and Bowen, 2006). These unusual waters have salinities that in all but a few cases are 5 to 10 times greater than seawater (Bowen and Benison,

† Corresponding author: e-mail, lamunk@uaa.alaska.edu
*Present address: 11 Cold Brook Rd., Randolph, NH 03593, USA.

2009). These studies further demonstrate that the fluids are Na-Cl and Na-Mg-Cl-$SO_4$ brines, the majority of which have a pH <4. Although extreme weathering and evaporation have played critical roles in the development of these brines, their Li content is quite low. Only a single brine sample exceeds 1 mg/L Li, and the vast majority of brines contain less than 0.5 mg/L (B. Bowen, pers. commun.) The climate and hydrology of these systems is favorable for enrichment of Li, but clearly a sufficient Li source and/or concentrating mechanism is absent.

Studies of continental Li-rich brines are most extensive for those in the Central Andes of Bolivia and northern Chile as reported in Risacher and Fritz (2009) and references therein. Hundreds of geochemical analyses for brines from this region are published by Moraga et al. (1974), Rettig et al. (1980), Risacher and Fritz (1991), and Risacher et al. (1999, 2003). The focus of most of this work was to examine the origin of the salts in the salars. Risacher and Fritz (2009) also provided a general classification for these brines (alkaline, sulfate-rich, and calcium-rich), and noted that alkaline salars are absent in Chile due to the presence of high-sulfur volcanic rocks that release hydrogen ions during weathering. The origin of solutes to salars in the Central Andes has been addressed by the major and trace element and isotopic investigations of Alpers and Whitmore (1990), Spiro and Chong (1996), Carmona et al. (2000), and Boschetti et al. (2007). However, none of these studies specifically addressed the origin and accumulation of Li. At Clayton Valley, Nevada, Kunasz (1974), Davis et al. (1986), Price et al. (2000), and Zampirro (2004) have explored the sources and concentrating processes of Li in the Clayton Valley brines. More recent work by Jochens and Munk (2011) and Munk et al. (2011) and current work by the authors of this paper on the Li-rich brines in Clayton Valley and the Salar de Atacama, Chile, is focused primarily on understanding the sources, transport, and accumulation of Li, and the age of the brines.

Bradley et al. (2013) identified common characteristics of Li-rich continental brines as the basis for an ore deposit model. In this paper, we elaborate on these common characteristics and focus on how they can be used as general exploration guidelines for locating future Li brine deposits on a global scale. We also include a discussion of the general geology, hydrogeochemistry, and climate of Li-rich brine systems followed by detailed discussion in the form of two case studies from the Salar de Atacama, Chile, and Clayton Valley, Nevada, which are currently two of the most well-studied Li-rich brine systems.

## Six Characteristics Common to Continental Lithium Brines

The Li-rich brine systems in our compilation (Table 1) share six common (global) characteristics that provide clues to deposit genesis while also serving as exploration guidelines. These include: (1) arid climate; (2) closed basin containing a salar (salt crust), a salt lake, or both; (3) associated igneous and/or hydrothermal activity; (4) tectonically driven subsidence; (5) suitable Li sources; and (6) sufficient time to concentrate Li in the brine. Table 1 summarizes information related to the six common characteristics of continental Li-rich brines.

Climate is the first characteristic and is perhaps the most important, as it is linked to all the others because it (1) contributes to the formation of the salars in a closed-basin setting, (2) is a factor in the concentration of Li in brines over time, and (3) is essential for the concentration of Li in evaporation ponds for economic purposes. Table 1 indicates the classification of the climate for each Li-rich brine location in terms of hyperarid, arid, or semiarid.

The second characteristic, shared by all continental Li-rich brines, is a closed basin with a salar(s) or salt lake(s). This characteristic is controlled primarily by climate and tectonic setting. Salars or salt crusts are common where brines exist in shallow subsurface aquifers. The aquifers may be composed of halite and other interbedded salts—commonly gypsum, as well as volcanic ash or ignimbrites, alluvial gravels and sands, and tufa (commonly evidence of modern or past hydrothermal activity). Most of the locations in Table 1 are classified as salars. Salt lakes may also contain enrichments of Li, although these are typically in the lower range of the concentration spectrum and there are only a few (Table 1) considered here. Most salt lakes do not produce Li because of low concentrations.

The third characteristic is evidence of hydrothermal activity. This likely plays a significant role in the formation of Li-rich brines for several reasons: (1) it provides a hot water source for enhanced leaching of Li from source rocks; (2) it is also likely a direct source of Li from shallow magmatic brines and/or magmatic activity; (3) it may play a role in the concentration of Li through distillation or "steaming" of thermal waters in the shallow subsurface; (4) thermally driven circulation may be an effective means for advecting Li from source areas to regions of brine accumulation; and (5) it can result in the formation of the Li-rich clay mineral hectorite, which can in turn be a potential source of Li to brines if leaching and transport occur from the clay source.

A fourth characteristic of all Li-rich brine deposits is that they occur in basins that are undergoing tectonically driven subsidence. The basins listed in Table 1 have a number of different tectonic drivers, including extension, transtension, and orogenic loading. In contrast, significant Li brine accumulations have not been reported from intracratonic basins in arid regions, such as the shallow sabhkas that rest on Precambrian basement of Australia or North Africa.

The fifth characteristic or requirement for the formation of Li-rich brines is a viable source(s) of Li. Lithium sources in various basins appear to include magmatic fluids, high-silica vitric volcanic rocks, hectorite, and ancient salt deposits. These along with the "time factor," discussed below, are probably the least well understood of the six characteristics. Despite the observation that multiple potential sources of Li exist they are yet to be definitively identified and quantified.

The sixth characteristic or requirement for the formation of Li-rich brines is time. The time it takes to leach, transport, and concentrate Li in continental brines is not well understood. However, it appears that most Li brines of economic interest are geologically young (Neogene). Currently we are working on dating the brines at Clayton Valley, Nevada, United States, and the Salar de Atacama, Chile, as well as developing hydrogeologic models for these environments to understand the transport and accumulation of Li in the closed basins. These studies will be the first to address the time factor for Li brines using a quantitative approach.

*General geology of Li brines (basins, tectonics, and stratigraphy)*

Figure 1 shows the global distribution of the locations of Li brines or salt lakes detailed in Table 1. We include the best known brines from North America, South America (Argentina, Bolivia, and Chile), and Asia (China) that are enriched in Li, irrespective of whether the brines are in production or not. Other well-known brines that contain Li include those with relatively lower Li concentration in lakes such as Great Salt Lake, Searles Lake, and the Dead Sea (Table 1), as well as oil field brines such as that from the Smackover Formation (Gulf Coast, United States) or the Devonian strata of the northeastern United States.

The majority of important Li-rich brines are located in the Altiplano-Puna region of the Central Andes of South America. Houston et al. (2011) classified the salars in the Altiplano-Puna region of the Central Andes in terms of two end members, "immature clastic" or "mature halite," primarily using (1) the relative amount of clastic versus evaporite sediment; (2) climatic and tectonic influences, as related to altitude and latitude; and (3) basin hydrology, which controls the influx of fresh water. The immature classification refers to basins that generally occur at higher (wetter) elevations, contain alternating clastic and evaporite sedimentary sequences dominated by gypsum, have recycled salts, and a general low abundance of halite. Mature refers to salars in arid to hyperarid climates, which occur in the lower elevations of the region, reach halite saturation, and have intercalated clay and silt and/or volcanic deposits. An important point made by Houston et al. (2011) is the relative significance of aquifer permeability which is controlled by the geological and geochemical composition of the aquifers. For example, immature salars may contain large volumes of easily extractable Li-rich brines simply because they are comprised of a mixture of clastic and evaporite aquifer materials that have higher porosity and permeability.

Our conceptual model for Li brines is shown in Figure 2. The model seeks to account for the sources, sinks, and processes that mobilize, sequester, and concentrate Li. This model is developed primarily from the information we have gathered over the past few years on the brines at Clayton Valley, Nevada, United States, and Salar de Atacama, Chile, which are further described in the following sections. The concepts of Houston et al. (2011) are specific to the range of salars observed in the Altiplano-Puna region of the Central Andes and are not necessarily transferable, in a global sense, to other Li-rich brines. Our conceptual model captures the framework of Houston et al. (2011), albeit with less specificity. We also recognize the earlier summaries by Asher-Bolander (1982, 1991), which describe a model for the formation of Li-rich clays and provide a brief description of factors contributing to the formation of Li-rich brines, in particular emphasizing the importance of hydrothermal activity in concentrating Li.

*Effects of geochemistry, climate, and hydrogeology on evolution of the Li brine resource*

*Geochemical characteristics:* The minimum, maximum and average Li concentrations for the brines and lakes in this study are listed in Table 1. These values are compiled from various sources detailed in Appendix 1. Because some of the basins do not have minimum and maximum Li concentration data reported in the literature we use the average Li concentrations to compare basins. The lowest average Li concentration is 10 mg/L in Searles Lake, California, and the highest average Li concentration is 1,400 mg/L for the brine in Salar de Atacama, Chile. Average seawater contains 0.2 mg/L Li.

The potentially important sources of Li to brines include high-silica volcanic rocks, preexisting evaporites and brines, hydrotherm clays, and hydrothermal fluids. The relative role of Li leaching from source rocks by low- and high-temperature fluids versus Li sourced in magmatic fluids themselves is not known and studies addressing this topic are scant. A study by Price et al. (2000) suggests that Li in the Clayton Valley, Nevada, brine is leached by groundwater from volcanic tuffs and that process alone can account for all the Li in the brines. However, experimental weathering studies by Jochens and Munk (2011) have shown that less than 10 $\mu$g/L Li are released from these volcanic rocks when exposed to water at ambient conditions. Godfrey et al. (2013) reported similar findings from low-temperature leaching of Li from volcanic rocks near Salar del Hombre Muerto, Argentina. Risacher and Fritz (2009) concluded that Li and B in Andean salars are derived from the weathering of ignimbrites. Yu et al. (2013) demonstrated that playas in the Qaidam basin receive Li transported by streams that is ultimately sourced from upstream hydrothermal inputs. They also hypothesized that source(s) of Li are from alteration of volcanic rocks by hydrothermal fluids and/or from direct connection to differentiated magmatic sources. Hofstra et al. (2013) reported that fluid inclusions in quartz phenocrysts from high-silica volcanic rocks in the Great Basin region of the United States contain elevated Li concentrations relative to their host vitric matrices, suggesting that volcanic glass is a significant and readily available source of Li released to the environment via weathering processes and that fluid inclusions in erupted volcanic rocks may ultimately be an important Li source.

The predictive sequence of evaporite formation in closed-basin salt lakes was established by Hardie and Eugster (1970) and Eugster and Hardie (1978). Their model indicates that there are three major fluid pathways or "chemical divides" that result during evaporation, which are dictated by the initial ionic composition of the fluid. Here we summarize the essence of their models in order to set a context for Li-enriched brines, but the reader is referred to Eugster (1980), Eugster and Hardie (1978), and Hardie and Eugster (1970) for more details. Path 1 occurs when there is an excess of bicarbonate compared to the alkaline earth elements (referred to as "soft water"), which produces the typical precipitation path from calcite to trona with no gypsum because the parent water is low in Ca and Mg. Examples from Eugster (1980) include Alkali Valley, Oregon, and Lake Magadi, Kenya. The Wilkins Peak member of the Eocene Green River Formation in southwestern Wyoming contains 25 major trona beds and is an example of a large volume geologic trona deposit. Path 2 occurs when there is an excess of alkaline earth elements compared to bicarbonate (referred to as "hard water") and in this case gypsum is precipitated after calcite and the path divides into a sulfate-rich system such as Saline Valley, California, or sulfate-poor system such as Bristol Dry Lake,

Table 1. Summary of Lithium

| Basin | Region | Lat. | Long. | Min Li (mg/L) | Max Li (mg/L) | Avg Li (mg/ L) | Li nearby hot springs (mg/L) | Total Li resource (Mt) | Mean annual temp (°C) | Precip. (mm/yr) |
|---|---|---|---|---|---|---|---|---|---|---|
| Clayton Valley | Nevada | 37.76724 | –117.58481 | 100 | 300 | 160 | 40 | 0.3 | 13 | 122 |
| Searles Lake | California | 35.73175 | –117.32930 | 10 | 80 | 65 | NA | NA | 19.5 | 85 |
| Salton Sea | California and Mexico | 33.25239 | –115.71031 | 100 | 400 | 200 | 5–100 | 0.316 | 22.7 | 65 |
| Great Salt Lake | Utah | 41.25311 | –112.70506 | 18 (north) 40 (south) | 43 (north) 64 (south) | 52 | 1.8-6.5 | 0.53 | 10.5 | 186 |
| Dead Sea | Israel | 31.15663 | 35.43786 | NA | NA | 10 | very low | NA | 16.7 | 58 |
| Salar de Atacama | Chile | –23.50069 | –68.24984 | 900 | 7,000 | 1,400 | 40 (El Tatio) | 6.3 | 13.9 | 39 |
| Salar de Maricunga | Chile | –26.93605 | –69.06936 | NA | NA | 920 | NA | 0.22 | 6.6 | 52 |
| Salar de Surire | Chile | –18.83700 | –69.005 | NA | NA | 340 | 8.3 | NA | 3.8 | 247 |
| Salar del Hombre Muerto | Argentina | –25.38555 | –67.13364 | 190 | 900 | 521 | 3.2-5.5 | 0.8 | 6.7 | 91 |
| Salar del Rincon | Argentina | –24.07478 | –67.08165 | NA | NA | 400 | 1,500 | 0.223 | 8 | 61 |
| Salar de Olaroz and Salar de Cauchari | Argentina | –23.45187 | –66.68484 | 282 (Olaroz) 200 (Cauchari) | 1,207 (Olaroz) 2,150 (Cauchari) | 650 (Olaroz) 510 (Cauchari) | NA | 0.9–1.0 | 7.2 | 90 |
| Salar de Llullaillaco (Mariana) | Argentina | –24.80602 | –68.29033 | 250 | 650 | 450 | NA | NA | 7.8 | 30 |
| Salar de Uyuni | Bolivia | –20.15888 | –67.56912 | 80 | 1,150 | 321 | NA | 10.2 | 9.3 | 62 |
| Salar de Copaisa | Bolivia | –19.36163 | –68.16860 | NA | NA | 243 | NA | NA | 8.1 | 320 |
| Salar de Pastos Grandes | Bolivia | –21.64429 | –67.79809 | 353 | 1,787 | 1,062 | 5.2 (edge) 67 (playa) | NA | 4.1 | 57 |
| Taijanier (Taijner) Lake | Qaidam, China | 37.49260 | 93.95323 | NA | NA | 290 | NA | 2.02 | 4.2 | 167 |
| Zhabuye Lake | Tibet, China | 31.34586 | 84.04752 | 500 | 1,000 | 680 | NA | 1.53 | 0.2 | 287 |
| Dangxiongcuo (DXC) | Tibet, China | 31.57053 | 86.73580 | NA | NA | 430 (5) | NA | 0.181 | 0.5 | 184 |

Notes: APVC = Altiplano-Puna volcanic complex, NA = not available
[1] All references for data in this table are detailed in the Appendix
[2] See Appendix for additional details on tectonics and geologic setting

California (Eugster, 1980). Path 3 is considered intermediate and describes waters with neither a dominance of bicarbonate nor the alkaline earth elements, which result in the formation of alkaline earth carbonates. In this case Mg is concentrated over Ca in the water and high Mg calcite or dolomite can form. At some point either the alkaline earth elements or bicarbonate are exhausted and the brine composition moves toward the alkaline earth path or forms gypsum, respectively. The gypsum path may follow either a sulfate-rich or -poor pathway (Eugster, 1980). These pathways control major element brine evolution through mineral precipitation, depending on the starting composition of the fluids. These three pathways can account for the majority of brine compositions indicating that closed basin brine composition is, on a first order, controlled by the composition of input waters. After precipitation of the alkaline earth elements, the brines are enriched in the alkali metals with a mixture of anions. Eugster (1980) noted that if the alkalis (Na and K) are treated separately, minor constituents and Si are included and the sulfide-sulfate equilibriums are considered, then other mechanisms in addition to mineral precipitation are required to account for the observed differences between inflow and brine waters. This led Eugster and

Brine Basins and Characteristics[1]

| Evap (mm/yr) | Aridity index | Aridity class | Min elevation (m) | Max elevation (m) | Relief (m) | Basin floor area (km²) | Basin area (km²) | Tectonic setting[2] |
|---|---|---|---|---|---|---|---|---|
| 1,425 | 0.0856 | Arid | 1,297 | 2,841 | 1,544 | 97 | 1,437 | Basin and Range extensional province; between Neogene core complex and its breakway zone |
| 1,659 | 0.05 | Arid | 482 | 1,984 | 1,502 | 187 | 1,891 | Basin and Range extensional province |
| 1,842 | 0.0336 | Arid | –71 | 3,497 | 3,568 | 972 | 20,051 | Pull-apart basin along intracontinental portion of San Andreas transform fault |
| 1,156 | 0.1428 | Arid | 1,281 | 3,959 | 2,678 | 18,075 | 86,896 | Basin and Range extensional province |
| 1,467 | 0.0343 | Arid | –415 | 2,805 | 3,220 | 1,111 | 43,272 | Pull-apart basin along intracontinental portion of Dead Sea transform fault |
| 1,440 | 0.0326 | Arid | 2,302 | 6,208 | 3,906 | 2,115 | 15,659 | Volcanic arc, plateau margin basin, active subsidence, ~6 km of Cenozoic strata |
| 950 | 0.0554 | Arid | 3,748 | 6,695 | 2,947 | 136 | 2,421 | Volcanic arc, high-elevation plateau margin basin |
| 1,100 | 0.2276 | Semiarid | 4,260 | 5,783 | 1,523 | 106 | 586 | Volcanic arc, high-elevation plateau margin basin |
| 1,106 | 0.0696 | Arid | 3,963 | 5,835 | 1,872 | 581 | 3,888 | Tectonic basin bound by crustal fault blocks, adjacent large silicic volcanic caldera, and resurgent dome dominate hydrographic basin |
| 1,233 | 0.0568 | Arid | 3,718 | 5,590 | 1,872 | 421 | 2,811 | Typical Puna, contractional basin and range, bound by crustal fault blocks and also by alluvium and volcanic edifices |
| 1,246 | 0.0707 | Arid | 3,886 | 6,136 | 2,250 | 480 | 5,699 | Typical Puna, contractional basin and range, bound by crustal fault blocks and also by alluvium and volcanic edifices |
| 1,148 | 0.0261 | Hyperarid | 5,755 | 6,648 | 893 | 128 | 1,234 | Volcanic arc, intra-arc basin |
| 1,318 | 0.0541 | Arid | 3,653 | 6,136 | 2,483 | 13,768 | 47,351 | Altiplano, low relief, minor volcanism, APVC to the south and thin skinned fold-thrust belt to the east |
| 1,316 | 0.2402 | Semiarid | 3,661 | 6,549 | 2,888 | 3,055 | 145,279 | Altiplano, low relief, minor volcanism, APVC to the south and thin skinned fold-thrust belt to the east |
| 1,094 | 0.0521 | Arid | 4,430 | 5,817 | 1,387 | 142 | 634 | Altiplano plateau, occupies an ~5.2 Ma caldera in the northern APVC |
| 989 | 0.0313 | Arid | 2,686 | 6,824 | 4,138 | 210 | 34,148 | Growth syncline within intracontintal foreland basin in the far field of the Himalayan-Tibet collisional orogen |
| 750 | 0.3333 | Semiarid | 4,424 | 6,580 | 2,156 | 3,055 | 16,768 | Neogene rift oriented at a high angle to the orogenic grain in the upper plate of the Himalayan Tibet collisional orogen |
| 783 | 0.2868 | Semiarid | 4,464 | 6,308 | 1,844 | 54 | 906 | Neogene rift oriented at a high angle to the orogenic grain in the upper plate of the Himalayan Tibet collisional orogen |

Jones (1978) to propose five major fractionation mechanisms that could account for brine evolution, including mineral precipitation, dissolution of efflorescent crusts and sediment coatings, sorption, degassing, and redox.

The world's most enriched Li brines appear to correspond to the late-stage fluids in the model of Eugster and Hardie (1978). For example, the Li-rich brine at Salar de Atacama, Chile, contains on average 1,400 mg/L Li with a minimum of 900 mg/L and a maximum of nearly 7,000 mg/L, and it is produced from a halite aquifer with carbonate and sulfate flanking the basin. This indicates that carbonate and sulfate mineral precipitation may have played a role in producing the existing Na-Cl brine that is enriched in Li.

In addition to evaporative concentration processes as described above, the distillation of Li from geothermal heating of fluids may play a significant role in concentrating Li in these brines, and perhaps causes prolonged replenishment of brines that are in production. Since many of the Li-rich brines exist over, or in close proximity, to relatively shallow magma chambers it may be that through faults and fractures, the late-stage magmatic fluids and vapors have pathways to migrate into the closed basins.

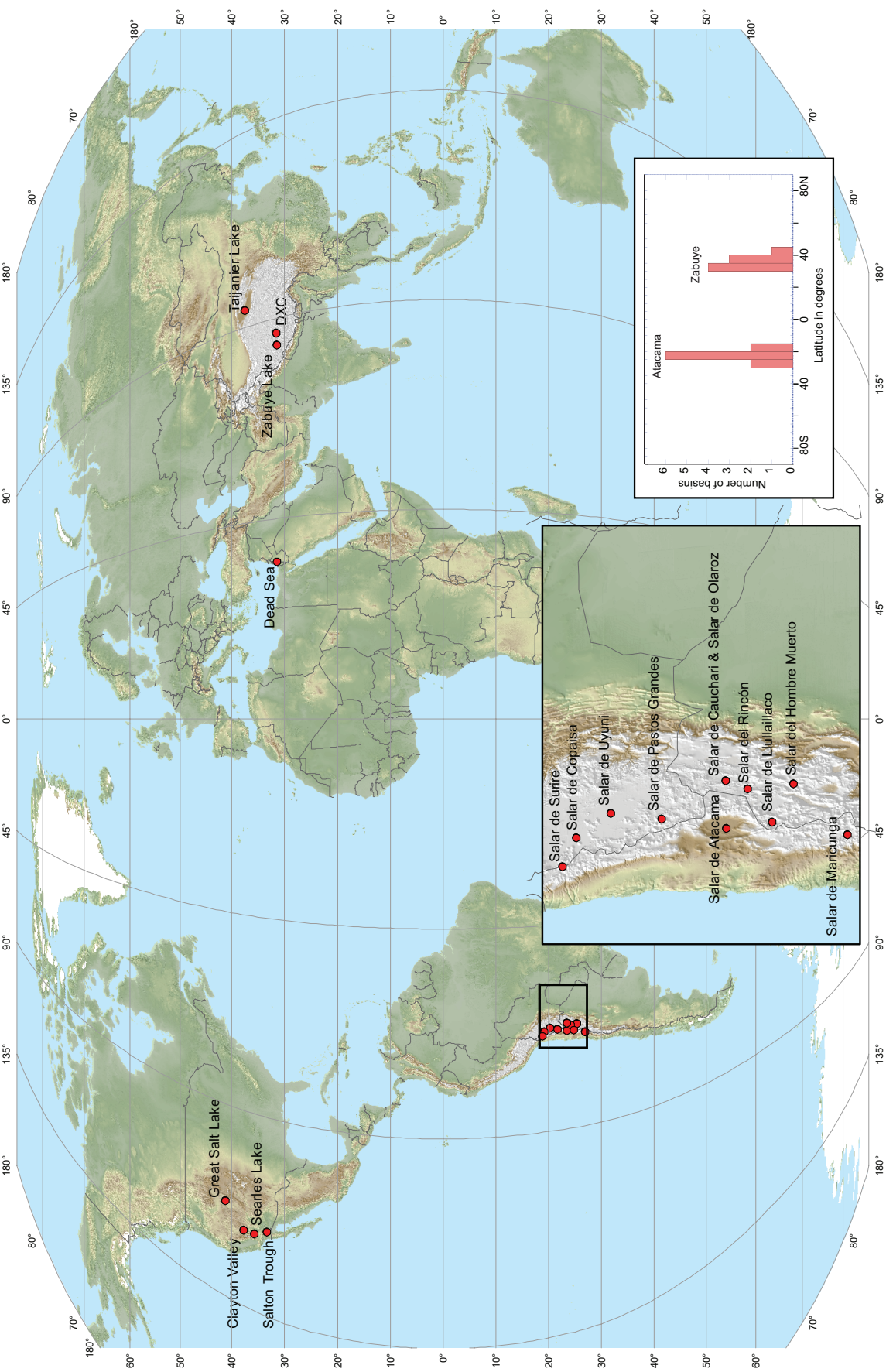


Fig. 1. World map of lithium brine deposits with inset showing detail in South America. Histogram showing the bimodal latitudinal distribution of Li brine deposits in northern and southern arid belts (adapted from Bradley et al., 2013).

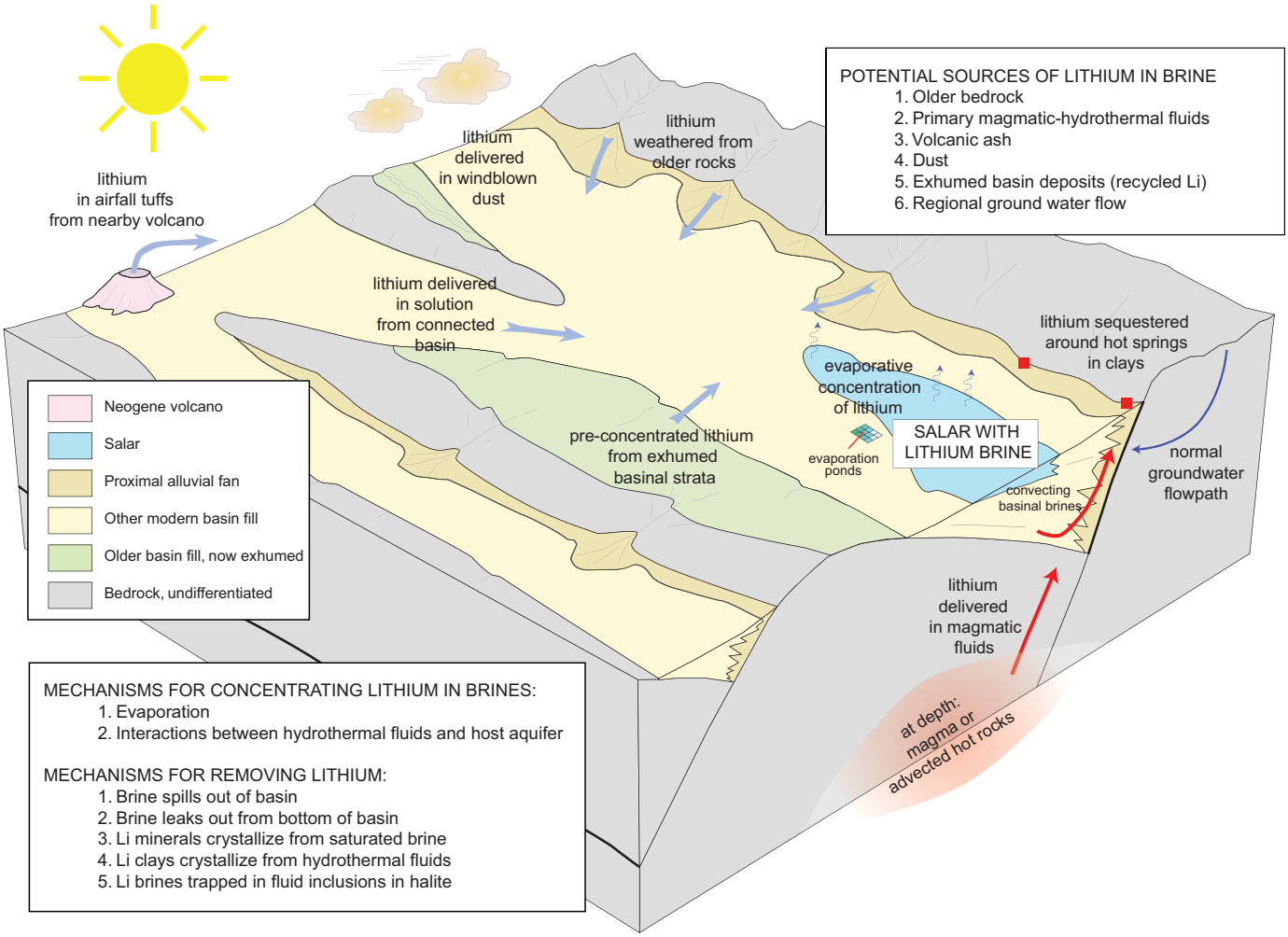


Fig. 2. Summary diagram of the geologic, geochemical, and hydrogeologic features of lithium brines emphasizing the sources, transport, and fate of lithium (adapted from Bradley et al., 2013).

*Climatic factors in the generation of Li brines:* Certain climatic characteristics are shared by all basins hosting Li-rich brines. Typically these basins are in subtropical and midlatitudes where arid climates are expected (Fig. 1). An arid climate is imperative for evaporative concentration of surface and shallow subsurface brines. Indeed, all of the basins investigated herein have evaporation far exceeding precipitation (Table 1; aridity index). As a first assessment, arid climate and a low precipitation/evaporation ratio are very favorable for the development of Li-rich brines. However, what is critical for generating economical brines is a large flux of water to the basin—seemingly at odds with the importance of arid climates in generating Li-rich brines. For example, on the Salar de Atacama evaporation greatly exceeds precipitation , irrespective of whether precipitation estimates are 10 mm/a (Jordan et al., 2002a), 25 mm/a (Houston et al., 2011), 39 mm/a (Table 1), or anything <50 cm/a (e.g., Bookhagen and Strecker, 2008). Under any scenario there is a net water deficit on the Salar de Atacama and evaporative concentration of inflow waters is possible, but without significant inflow water it would be impossible to generate the enormous volume of highly concentrated brine present there.

The magnitude of water flux through an Li-rich brine-generating basin that is necessary for economical brines is dependent, in turn, on the Li content of the average inflow waters. Economical Li brines contain a minimum of 100 mg/L Li, and more commonly 500 to 5,000 mg/L Li, whereas the inflow waters may only contain Li in the range of 1–10 mg/L or less. Therefore, at an absolute minimum, inflow waters must be concentrated by one full order of magnitude. Given that most Li brine-generating basins have many inflows that are not enriched in Li, it is assumed that the average Li content of inflow waters is less than 1 mg/L Li. Thus, the combined effects of evaporation and precipitation of evaporite minerals must concentrate inflow waters by many orders of magnitude and the time-integrated flux of water through the basin must be sufficient to create a Li brine deposit that contains enough total Li to be economical, irrespective of Li concentration.

There are a number of ways in which large influxes of water can be combined with high evaporation rates to create favorable conditions for generation of Li-rich brines. One example is that of a seasonal climate where wet seasons alternate with hot and dry conditions. To generate both sufficient inflow and evaporation with seasonal climatic variation, each year

must be split between one of these two functions. Essentially the recharge area (precipitation) and the concentration area (evaporation) are identical, but they must each serve these functions for only a part of the year; thereby increasing the amount of time required to generate a brine of given Li concentration. Similarly, alternating between wet and dry climates on longer (climatic) timescales is a possible mechanism for evaporative concentration of large volumes of water in a closed basin. Again, time is the limiting factor in this scenario as the same land surface must serve both functions. Climatic cycles likely played an important role in the generation of the Li-rich brine in Salars de Copaisa and Uyuni, where at least 130 ka of climatically driven lake-level cycles have been documented on the Bolivian Altiplano (Placzek et al., 2011). Alternatively, recharge and evaporative concentration can operate simultaneously in different areas of the hydrographic basin. As for the Salar de Atacama, precipitation elsewhere in the drainage basin can serve as the Li influx while the low-elevation salar surface can serve to concentrate the inflow waters. Likewise, the nearly 5,900-m-high resurgent dome of the Cerro Galán caldera may be an important recharge area for the Salar del Hombre Muerto at ~4,000-m elevation.

In addition to elevation differences, the size of a drainage basin relative to the salar/playa surface is an important consideration (Table 1). Importantly, the size of the drainage basin is not limited to surface drainage. Regional groundwater flow below topographic divides is one additional factor that can contribute significant amounts of water to a closed basin. For example, at Clayton Valley, Nevada, a large regional groundwater flow system contributes the majority of the water flux to the basin (Rush, 1968; Belcher, 2004). Subsurface flow paths provide ample water to aid in mobilization and evaporative enrichment of Li within a closed basin and may also provide significant additional sources of Li.

The climatic condition requisite for generation of Li brines is a net water deficit at the basin floor. A wide range of localities satisfy this condition; however, water cannot be evaporated and Li cannot be concentrated unless there is a sufficient influx of both. For this reason, localities favorable to generation of Li-rich brines juxtapose wetter conditions with the hot, dry conditions characteristic of basin floors. This can be accomplished many ways, including seasonality, climatic cycles, and climatic variation within the surface and/or subsurface drainage basins. Therefore, the role of climate can be complicated by other factors and these must be assessed for each basin.

*Hydrogeology.* As discussed above most known Li brine deposits occur in the shallow subsurface of tectonically active, closed basins in arid regions (Fig. 1). In these settings, basin hydrology and hydrogeology are inextricably linked through depositional and tectonic processes and have important impacts on the geometry and nature of subsurface flow paths. Host aquifers in these systems range from clastic sedimentary units associated with alluvial fans and playa sediments (including volcanic deposits) to halite and other salts. Fresh water enters the system either on the flanks through permeable alluvial sediments and is confined to the more permeable facies (fan gravels, sands), or through subsurface paths from upgradient basins. Fresh water mixes and floats on the denser basin brines and is ultimately driven upward by a moisture gradient which is maintained by sufficiently arid conditions. This results in significant loss of water through evaporation and concentration of dissolved constituents.

Lithium can enter a basin from leaching of rocks and alluvial fans and hydrothermal fluids associated with magma at shallow depths. Many closed basins are actually connected via subsurface flow paths and can act as sinks for regional transport of ground water. Large fault systems can often act as preferential flow paths allowing Li to be delivered via magmatic-derived fluids from depth. Because brines have extremely high total dissolved solids, they are denser than fresh water, which affects the movement of these fluids in the subsurface. Often there are strong feedbacks between the dissolution of halite, moving ground water, and density changes resulting in complex flow paths that act to mix subsurface fluids. Through a combination of evaporation and hydrothermal distillation brines can reach Li concentrations on the order of 1,000s of mg/L.

The permeability of the host aquifer for the brine plays an important role in the development of and exploitation of the resource. Immature salars, those with significant clastic sediments (Houston et al., 2011) have porosity and permeability dominated by primary depositional processes. Coarse-grained sediments tend to accumulate at the margins of the basin and commonly fine upward and basinward. These sediments have high permeability and well-connected porosity. Clastic sediments at the center of the basin, such as lacustrine facies, commonly have high porosity but low permeability. These sediments often have intercalated evaporite deposits that act as confining units to brines deeper in the basin. Mature salars are dominated by evaporite deposits that have little connected primary porosity. Brines in these environments tend to be transported and hosted in fractures and dissolution features that vary in occurrence in both time and space. The spacing of these features is small (<1 m) such that the shallow evaporite aquifers can be treated as a well-connected porous medium at the km scale. These aquifers often exhibit strong depth dependence in hydrologic characteristics, where the higher porosity and permeability are located closer to the land surface.

## Lithium Brine Case Studies

### *Case study 1: Clayton Valley, Nevada*

Clayton Valley is located in Esmeralda County, Nevada, United States, approximately 160 km north of Death Valley, California (Fig. 3) and is the location of the only Li-rich brine deposit in production in North America. Clayton Valley is a closed basin with an area of 1,342 km$^2$ and a playa surface of 72 km$^2$. The basin lies in the eastern rain shadow of the Sierra Nevada Mountains and is arid with an annual average precipitation of about 12 cm, average evaporation rates of 142 cm/yr, and an average temperature of 13°C. The elevation of the valley floor is 1,298 m, lower than any of the adjacent basins.

The basement consists of late Neoproterozoic to Ordovician carbonate and clastic rocks that were deposited along the ancient western passive margin of North America. During late Paleozoic and Mesozoic orogenies, the region was shortened and subjected to low-grade metamorphism (Oldow et

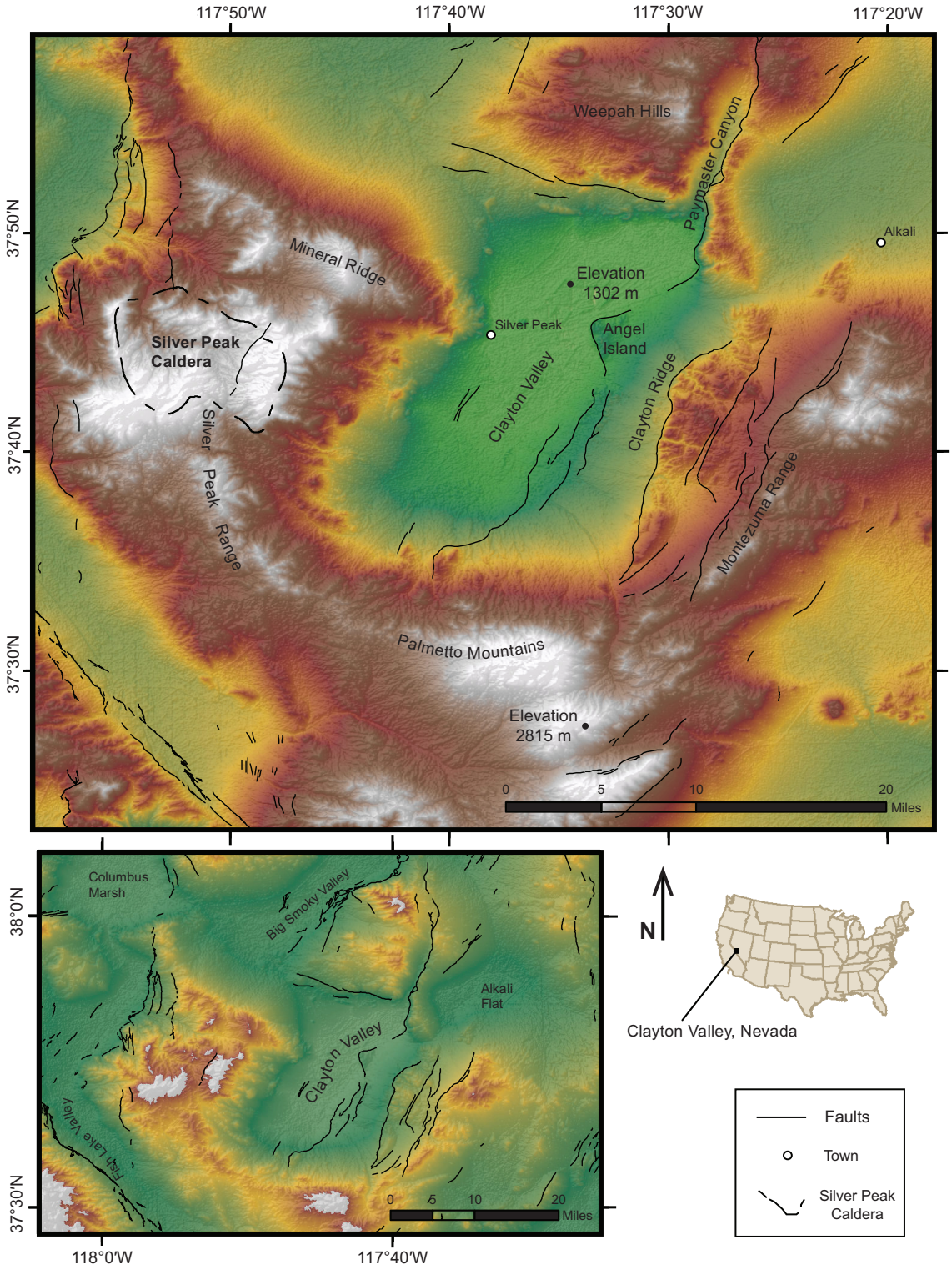


Fig. 3. Shaded relief map of Clayton Valley, showing major features noted in text and Appendix. Fault locations from U.S. Geological Survey (ftp://hazards.cr.usgs.gov/maps/qfaults) and the location of the Silver Peak caldera is from Robinson (1972).

al., 1989). Granitoids were emplaced at ca. 155 and 85 Ma. Extension commenced at ca. 16 Ma and has continued to the present, with changes in structural style. A metamorphic core complex just west of Clayton Valley was exhumed from midcrustal depths during Neogene extension. The basin is bounded to the east by a steep normal fault system toward which basin strata thicken. Late Miocene to Pliocene tuffaceous lacustrine facies (Esmeralda Formation of older usage from Albers and Stewart, 1972) contains up to 1,300 ppm Li and an average of 100 ppm Li (Kunasz, 1974; Davis and Vine,

1979). Miocene silicic tuffs and rhyolites along the basin's eastern flank have Li concentrations as high as 228 ppm (Price et al., 2000). Multiple wetting and drying periods during the Pleistocene resulted in the formation of lacustrine deposits, salt beds, and Li-rich brines. Hectorite in the surface playa sediments contains from 350 to 1,171 ppm Li (Kunasz, 1974). Prior to development of the brine resource, a salt flat and brine pool existed in the northern part of the basin, but groundwater pumping has eliminated the surface brine pool.

At Clayton Valley, brines are pumped from six aquifer units (Zampirro, 2004). Volcanic glass in the main ash aquifer shares strong compositional affinities with the ~760-ka Bishop Tuff. However, this ash bed could also be correlated with some of the 0.8 to 1.2 Ma tuffs of Glass Mountain (Sarna-Wojcicki et al., 2005). In Clayton Valley, this aquifer system ranges between 5 to 20 m thick. Other aquifers (and their thicknesses) include the salt aquifer system comprised of thick-bedded halite deposits interbedded with silt (30–100 m); the tufa aquifer system, an aquifer of consolidated travertine in the uppermost strata localized in the northeastern part of the basin (6–20 m); the lower ash system, an extensive zone of thin volcanic ash deposits, interbedded with silt and sand (10–90 m), also exposed in outcrop in the basin; the marginal gravel aquifer, a localized aquifer of mixed gravel, sand, and silt along the eastern margin of the basin (10–70 m); and the lower gravel aquifer, a poorly sorted deposit of coarse to fine gravel, sand, and silt at ~1-km depth (50–100 m).

The Li content of the waters in Clayton Valley ranges from less than 1 $\mu$g/L in snow up to 407 mg/L in groundwater from one of the aquifers composed of volcanic ash. The cold springs surrounding Clayton Valley have Li concentrations of less than 1 mg/L. One hot spring in the area located east of Clayton Valley near Alkali, Nevada, contains 1.6 mg/L Li. Lithium content of the groundwater from a freshwater well in an alluvial fan located near Silver Peak, Nevada, is less than 1 mg/L. Two groundwaters, one located just north of the town of Silver Peak and the other on the far northeast part of the basin, contain about 40 mg/L Li.

Davis et al. (1986) proposed that the Li at Clayton Valley, Nevada was concentrated by the same processes as Cl and therefore must have been trapped as an Li-rich fluid when the halite formed. They also hypothesized that in the last 10,000 years meteoric water entered the basin and dissolved the halite to form brines with evaporative signatures. Munk et al. (2011) indicated that other sources and processes were likely involved in the formation of the brines in the system because nonhalite aquifers produce brine with higher Li concentrations than the halite aquifer. It may be that a combination of hydrothermal activity and leaching from volcanic ash and clays are major sources of Li in the aquifers in Clayton Valley, Nevada. We have found that one of the aquifers composed predominantly of pumice ash has nearly identical major and trace element glass composition to the Bishop tuff; however, the Li content in glass from this aquifer is approximately 12 ppm higher (72 ppm) than the Bishop tuff from a number of other localities. This may be an indication that the volcanic glass in this aquifer exchanges Li over time.

Figure 4 indicates that snow, hot and cold springs, and cold groundwater in Clayton Valley are more dilute (have lower Na concentrations) than the hot groundwater and brines. Additionally, the cold springs have enriched $\delta$D values compared to the hot groundwater, most likely caused by evaporation at the surface. It appears that there are two mixing pathways that can account for the composition of waters in the basin (Fig. 4). We interpret these mixing lines as dilute inflow waters interacting and leaching chemical constituents from the rocks

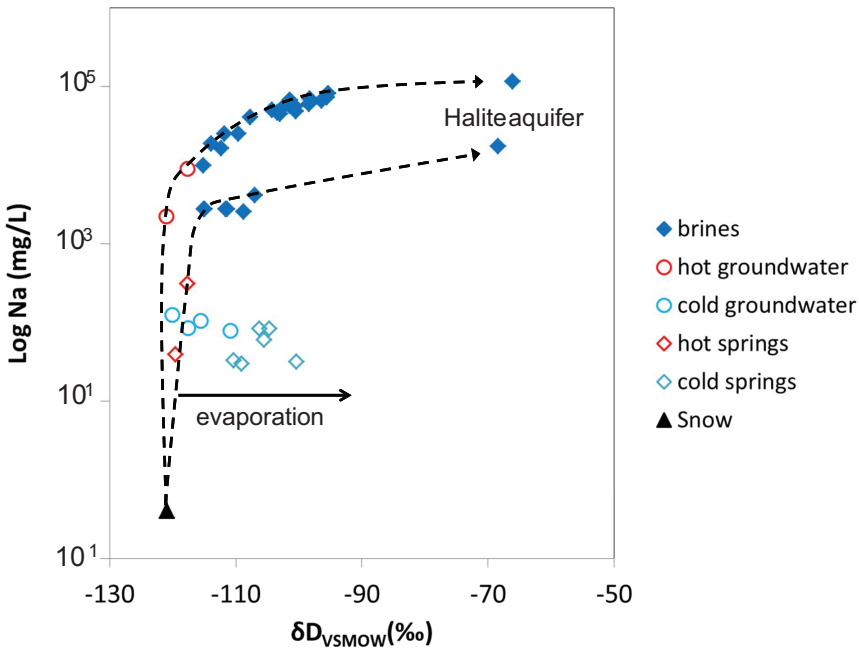


Fig. 4. Log Na vs. $\delta D_{VSMOW}$ for waters in the Clayton Valley, Nevada, basin. Cold shallow groundwaters and springs exhibit dilute concentrations and an evaporation trend as a function of increasing $\delta D_{VSMOW}$. Hypothetical mixing/evaporation curves are represented by dashed arrows from the meteoric water (snow) to brine in the halite aquifer.

in the basin with the possibility of hydrothermal inputs contributing water with higher total dissolved solids (TDS) to the brines. These processes could then be followed by mixing with other brines, concentration through evaporation, and/or halite precipitation to form the various brine compositions in the basin.

*Case study 2: Salar de Atacama, Chile*

The Salar de Atacama is a large closed basin which lies on the Tropic of Capricorn in the Atacama Desert approximately 200 km east of the Pacific Ocean and immediately to the west of the Altiplano-Puna plateau (Fig. 5). The basin coincides with a sharp bend in the modern Andean volcanic arc which retreats 60 km east from its regional north-south trend. The salar has a surface area of 3,000 km$^2$ and a drainage basin flanked on all sides by substantial topography; the Andean volcanic arc dominates recharge to the salar. The salar surface is 2,300 m above sea level and is ~2,000 m lower than the volcanic arc on the western plateau margin. As in the rest of the Atacama Desert, precipitation on the salar surface is rare. The adjacent Andean highlands receive precipitation more often but are still arid to hyperarid (Strecker et al., 2007). Evaporation at the elevation of the salar varies between 0 to 2.8 mm/d, depending on the surface characteristics (Kampf et al., 2005); relative to an estimated mean annual precipitation of 39 mm, the P/E ratio (aridity index) is ~0.033. Interestingly, no evaporation was measured by Kampf et al. (2005) from the rough halite nucleus of Salar de Atacama that comprises approximately half of the surface area and hosts the Li-rich brine at 30-m depth.

Water in the Salar de Atacama basin and the adjacent Andean arc varies in Li concentration from approximately 0.05 to 5 mg/L in the Andean inflow waters, 5 to 100 mg/L in shallow groundwaters in the southern and eastern flanks of the basin, and up to 5,000 mg/L in brines. This indicates that the brines in the basin can be significantly more concentrated, by up to five orders of magnitude, compared to water entering the basin.

The geologic history of the Salar de Atacama basin can be summarized as follows. Sedimentary, volcanic, and plutonic rocks indicate its position during the Paleozoic along the western margin of Gondwana. During the Jurassic and Early Cretaceous this region was an extensional backarc basin, with inversion and basin-scale tectonic subsidence initiating in the Late Cretaceous. This continental backarc setting persisted through the Paleogene, transitioning to a forearc basin in the Neogene. Uplift and predominantly clastic deposition have been ongoing since the Cretaceous, and during the Plio-Pleistocene thick halite deposits have accumulated in the center of the basin.

Details of the Cenozoic geologic history highlight several relevant observations in the Salar de Atacama (additional details on the older geologic history can be found in the Appendix). There was first a foreland basin originating in mid-Cretaceous, with thrusting and coeval sedimentation occurring during the Cretaceous and Paleogene (Arriagada et al., 2006). During the Oligocene-early Miocene normal faulting, perhaps in a transtensional environment, controlled the western margin of the basin and accommodated thousands of meters of strata (Jordan et al., 2007). Much of this sedimentation was accommodated by a normal fault along the western basin margin with as much as 6 km of vertical displacement (Pananont et al., 2004). From ~12 Ma onward the volcanic arc was established east of the Salar de Atacama and shortening resumed, uplifting the intrabasinal Cordillera de la Sal and later resulting in development of blind thrust faults within the basin (Jordan et al., 2007). Interpretation of seismic data by Pananont et al. (2004) suggest that the Cordillera de la Sal, a prominent N-S-trending anticlinal feature that separates the Salar de Atacama from the Cordillera Domeyko, results from diapiric flow of Oligocene to middle Miocene strata initiated in the Miocene and is associated with a deep reverse fault. Following initiation of diapiric flow in the western Salar de Atacama basin, uplift of the Altiplano-Puna plateau is accommodated by monoclinal folding which is expressed in the geomorphology and westward tilted strata at the plateau margin (Jordan et al., 2010). A number of late Miocene and Pliocene ignimbrites derived from calderas on the plateau can be traced westward into the subsurface of the Atacama basin. These ingimbrites interfinger with halite deposits that are typically 1 km thick, and establish the age of these strata as Plio-Pleistocene with a lower age limit likely to be sometime in the late Miocene. In the southern portion of the salar these deposits are offset by the Salar fault system, which exhibits close to a kilometer of down-to-the-east offset on a reverse fault during this interval (Jordan et al., 2002b). The Salar fault system can be followed to the south-southwest into the Tilomonte (Tilocalar) Valley as moderate- to high-angle reverse faults which offset a Pliocene ignimbrite and Paleozoic rocks of the eastern Cordón de Lila. Some of the features of this fault system as exposed in the Tilocalar (Tilomonte) Valley suggest the influence of major pre-Andean basement structures (Kuhn, 2002).

Several aspects of this geologic history are relevant to the generation of Li-rich brine in Salar de Atacama. There are a number of fault systems with kilometers of offset, which may be crustal scale features and preferential flow paths for fluids. During the Miocene and Pliocene several voluminous ignimbrite pulses related to development of the large Altiplano-Puna volcanic complex indicate major magmatic activity to the east on the plateau (Salisbury et al., 2011). It is possible that this volcanism is intimately related to late Miocene uplift of the plateau via lower crustal delamination (cf. Hoke and Garzione, 2008). If large-scale tectonic factors play a role in the generation of Li brines these processes might be relevant to generation of the Li-enriched brine in Salar de Atacama, particularly if the mantle is considered to be the ultimate source of Li to brines. Crustal scale faults within the Atacama basin itself are not necessarily good candidates for communication between the mantle and brine aquifers in light of the fact that the lithosphere below the Atacama basin is widely believed to be a cold, rigid block on the basis of seismological data (Schurr and Rietbrock, 2004).

However, numerous faults exist between the salar and the magmatic arc in the southern half of the Atacama basin and these are more attractive fluid conduits. As their coincidence with young lavas and recent volcanic edifices document, magmatic fluids have exploited these faults as conduits. Further, these faults do not express themselves in the northern half of the basin and instead are confined to the portion of the basin that is known to exhibit the highest concentration Li brines

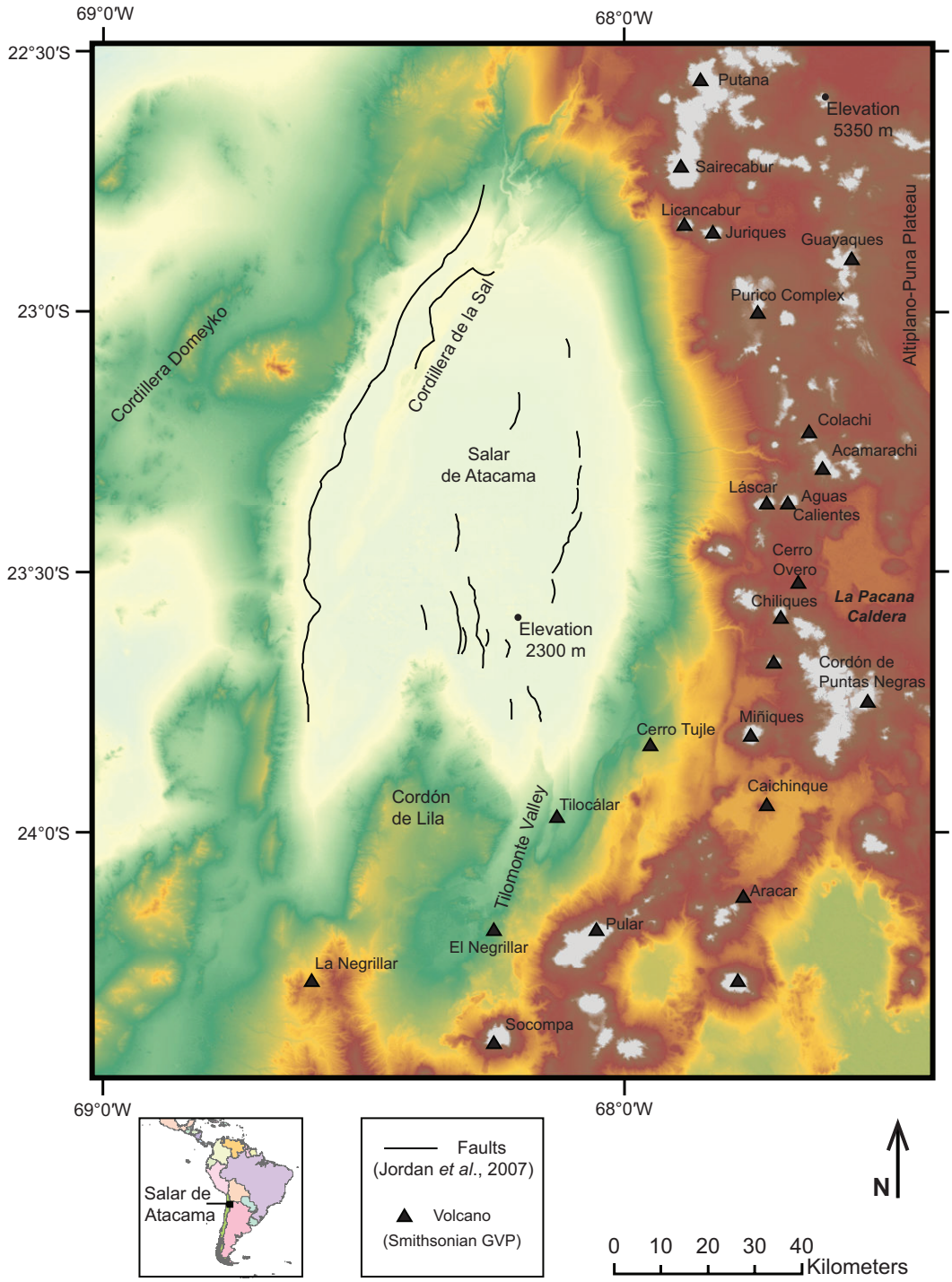


Fig. 5. Shaded relief map of Salar de Atacama, Chile, showing major features noted in text and Appendix. Fault locations from Jordan et al. (2007) and the Andean volcano locations are from the Smithsonian Global Volcanism Program (GVP; http://www.volcano.si.edu).

(Ide and Kunasz, 1989). We have observed high dissolved $^{3}He$ concentrations in shallow groundwater and brine in the southeastern part of the Atacama basin. These high $^{3}He$ concentrations have not been observed in water and brine sampled from the western half of the Atacama basin, and we interpret the $^{3}He$ as an indicator of the influence of mantle-derived gases in the southeastern sector of the basin.

The interaction of groundwater and magmatic systems in the Andean arc and on the Altiplano-Puna plateau is another potential mechanism for transporting Li, ultimately mantle derived, from volcanic systems to the Salar de Atacama. The huge volcanic centers of the Altiplano-Puna volcanic complex contain large volumes of highly evolved and low-temperature magma at shallow crustal levels; melt inclusion data demonstrate that

magmatic Li contents of 100 to 1,000 ppm are common in this region (Lindsay et al., 2001; Schmitt, 2001). Whether and how these magmatic systems are connected to the Salar de Atacama by thermal waters and the regional groundwater system remains a major question. Crustal-scale and smaller faults may serve either as conduits for or barriers to fluid flow (cf. Caine et al., 1996). Multiple ignimbrites exist at depth within the northern half of the basin. These interfinger with halite and are likely to be permeable enough to transport fluids, especially under the large topographic gradient along the western plateau margin. It seems conceivable to connect the giant magmatic systems of the Altiplano-Puna volcanic complex as a Li source to Salar de Atacama brines, but understanding of the regional groundwater systems at the plateau margin is limited. Jordan et al. (2002a, b) have proposed that the accumulation of halite in the Atacama basin is coincident with monoclinal folding, and uplift of the Altiplano-Puna plateau immediately to the east. Indeed, deep groundwater flow driven by the elevation contrast across the western plateau margin may be a consequence of plateau uplift and result in initiation of the thick halite sequence in the Atacama basin, but in order to evaluate this possibility much work characterizing the modern deep groundwater system is needed.

Certainly, Andean magmatic systems have a large role to play as Li sources either directly or indirectly via surface and subsurface weathering of silicic volcanic rocks. It is important to note that the rock units which comprise the Atacama basin and its strata control to a large degree the evolution and ultimate composition of brines. Bedrock and basinal strata of Salar de Atacama are essentially devoid of limestone, with the exception of Jurassic strata exposed in the Cordillera Domyeko (Flint et al., 1993) and minor Maastrictian(?) marine carbonates (Mpodozis et al., 2005). As described in previous sections, catchment lithologies control the chemical composition of inflow waters, volcanic sulfide results in sulfate-rich brines, and the dearth of limestone results in brines that are Ca-poor relative to sulfate. For this reason, the evaporite mineral sequence in the Atacama brines is prone to precipitate Mg and Li sulfate salts in the absence of Ca (Boschetti et al., 2007). This chemical divide (cf. Eugster and Hardie, 1978) has implications, not only for the evolution of brine chemistry but also for the logistics and economics of processing brines for Li.

Finally, the hydrographic history of the Salar de Atacama basin has implications for the origin and evolution of the Li-rich brine. It is possible that the basin has been closed continuously since the uplift of the Cordillera Domeyko in the Cretaceous, and almost certain that the basin has been hydrographically closed with respect to surface waters since the late Miocene. Jordan et al. (2007) suggested that the western margin of the modern basin was established by a major down-to-the-east normal fault during an Oligocene period of extension or transtension. Irrespective of the exact timing, any of these scenarios for hydrographic closure of the basin permit accumulation and concentration of brines on the timescale of 1 to 10 m.y. at a minimum.

## Lithium Uses, Demand, and Global Li Brine Resources

Lithium was not discovered until the early 1800s and was little more than a scientific curiosity at first. After many decades at low levels, Li production has increased exponentially since the 1950s (Mohr et al., 2010; Fig. 6), with more growth expected. Lithium is alloyed with other elements such as aluminum, cadmium, manganese, and copper to produce high strength-to-weight metals. It is used as a coolant in nuclear breeder reactors. Compounds of Li are used as heat-resistant glass, ceramics, and lubricants. It is the key ingredient of drugs used to treat bipolar disease. But the most important modern use of Li is in rechargeable Li ion batteries for cell phones, laptops, and hybrid and electric cars (Garrett, 2004). Lithium ion batteries are superior because they are lightweight and can be efficiently recharged. Lithium's use in cars is what gives it a key role in global efforts to reduce greenhouse gas emissions and minimize global warming.

Projections by Gruber et al. (2011) and Kesler et al. (2012) indicate that demand for Li will increase through the year 2100, with nonbattery, portable electronic batteries, and vehicle batteries each contributing to this demand. Depending on the global economic growth scenario adopted, and accounting for 90% recycling, they concluded that between 12 and 20 million metric tons (Mt) of Li will be needed. Global Li resources have recently been estimated by several authors. Gruber et al. (2011) estimated 39 Mt of Li metal; Tahil (2008) estimated 19.2 Mt; U.S. Geological Survey (2011) estimated 33 Mt; Evans (2010) estimated 34.5 Mt; and Yaksic and Tilton (2009) estimated 64 Mt. Barring major new uses for Li, global demand is unlikely to exceed supply in the next century.

### *Exploration for lithium-rich brine deposits*

*Identification of prospective basins:* All of the Li-rich brine basins in Table 1 are closed basins, and they are all marked by a saline lake or a salar (i.e., a salt flat or salt-encrusted depression). Closed basins form because of tectonics but they are maintained only where, over longer time-spans, evaporation exceeds precipitation. If the long-term rate of precipitation in a basin increases sufficiently, eventually lake water will overtop some point along the drainage divide and drain, carrying the dissolved Li away. Evidently, the aridity classification must be semiarid or drier, but the numerical aridity index for the basins in Table 1 ranges through an order of magnitude,

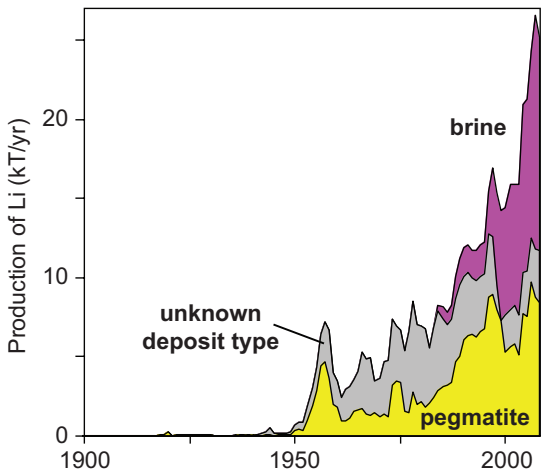


Fig. 6. Lithium production since 1900 (modified from Mohr, 2010).

from 0.03 to 0.33. Judging from the present-day distribution of basins, the favorable zones lie between about 19° and 37° north or south (Fig. 1). Rain-shadow effects probably stretch the north-south span of favorable latitudes. Mean annual temperature does not appear to be a critical factor, with values ranging through two orders of magnitude from 0.2° to 22.7°C.

All of the world's Li-rich brine basins cataloged in Table 1 are tectonically active, subsiding basins as evidenced by thick accumulations of Quaternary to recent sediment, and in most cases, also evidenced by faults with Quaternary to recent displacements. In contrast, shallow, internally drained depressions on the stable cratons (e.g., Australia: Benison and Bowen, 2006; Algeria: Hacini et al., 2008) do not appear to be prospective. Lithium-brine resources are found in a range of tectonic settings from extensional to strike-slip to contractional (Table 1, Appendix). The overall tectonic setting where Li-rich brines occur appears to vary and may not be the primary factor in determining favorability for Li-rich brines, although at the local scale, tectonics control basin geometry. Most of the Li-rich brine basins in Table 1 show evidence for elevated heat flow. The most obvious evidence includes young volcanoes, hot springs, and geothermal resources. Only one basin in our compilation, Lake Zabuye, appears to have none of these.

Evidence of older hydrothermal activity is seen in several instances and should be regarded as a favorable characteristic. For example, at Clayton Valley, Nevada, some Miocene to Pliocene basinal deposits were hydrothermally enriched in the Li-rich clay hectorite; this took place a few million years ago, before these altered strata were uplifted and exposed. Hectorite concentration halos have been reported from several basins that lack Li-rich brines in the U.S. Basin and Range province (Vine, 1980). In such cases, a hectorite halo may be all that remains of a former brine system that has since leaked away. Borate deposits appear to be hybrids involving both hydrothermal and evaporative processes; their presence is also a favorable indicator for Li brines. At Salar del Rincón, hot-spring deposits which appear inactive contain residual water with up to 1,500 mg/L Li (Toledo et al., 2009).

Source rocks such as felsic, vitric tuffs that have abundant and readily leached Li are favorable (Price et al., 2000) but perhaps not the sole source of Li as it is present in most crustal rocks at tens of parts per million. There are extensive ignimbrite deposits flanking the east side of the Salar de Atacama basin that can contain up to nearly 700 ppm Li in quartz melt inclusions (Lindsay et al., 2001). Similarly, in the western United States quartz inclusions from large silicic eruptions contain appreciable Li. Hofstra et al. (2013) have suggested that Li in melt inclusions is the best estimate of preeruptive magmatic concentrations and that subsequent loss of Li during eruption, lithification, and weathering of a moderate volume eruption is sufficient to generate an economical brine deposit if it can be efficiently mobilized and concentrated. If there are hydrothermal inputs of Li to the brines that are associated with silicic magmatic systems we would argue that this type of source has the potential to bring high concentrations of Li to the brine. It then becomes a question of how to get the Li-rich fluids from the hydrothermal source to the brine; this may occur along faults and fractures in the case of the Salar de Atacama system.

Physiographic aspects of Li-rich brine basins do not appear to be that important to the existence or size of the resource. Of the basins in Table 1, basin-floor areas range from 54 to 18,075 km$^2$, catchment areas range from 634 to 145,279 km$^2$, and basin-floor elevations range from –415 to +4,464 m. A special situation exists at Clayton Valley, Nevada, which may be partly responsible for the size of the resource. Clayton Valley is one of five adjacent closed basins. Although they are hydrologically unconnected at the surface, groundwater ultimately flows into Clayton Valley, the lowest elevation of the five (Zampirro, 2004). In fact Clayton Valley may be the end of very long regional groundwater flow paths in the western Basin and Range (Belcher, 2004, plate l).

*Basin-scale exploration:* Within a closed basin that is prospective for Li-rich brines based on the above criteria, the most convenient exploration tool is surface sampling of waters and/or sediments. Because many Li brines are located within 1 m of the surface salt crust, water sampling is relatively easy to use as a general exploration tool. However, for deeper brines it may be useful to perform geophysical surveys to identify high conductivity anomalies that could then be drilled for sampling.

Another exploration strategy is surface sampling of sediment. This approach, however, has produced mixed results. During reconnaissance exploration for Li resources by the U.S. Geological Survey in the 1970s, surface samples were analyzed from 41 closed basins in the U.S. Basin and Range Province. Whereas four basins were identified as having anomalous Li concentrations (defined as >300 ppm; Vine, 1980), neither Great Salt Lake Desert nor Searles Valley were found to be prospective by this measure, despite the known occurrence of Li brines at depth.

*Geologic reconnaissance:* Several important observations related to the youthfulness of a prospective basin and it's tectonic, sedimentary, and heat-flow characteristics can be assessed with a boots-on-the-ground approach. Basins likely to host Li-rich brines should include young high-silica volcanic rocks, evidence for Quaternary faulting, thick accumulations of clastic and/or evaporite strata, and hot-springs or hot-spring deposits. Given the observations of Hofstra et al. (2013) on the Li content of quartz melt inclusions versus host rocks, it is clear that whole-rock geochemistry of vitric rocks may be of limited value for exploration purposes. Rather, if much of this Li has already been mobilized an analysis of quartz-hosted melt inclusions in potential source rocks may be a better measure of whether the rocks are (were) a potential Li source. In addition heat flow can be assessed by estimating the temperatures of formation for hot-spring carbonates or by application of chemical thermometers to hot-spring water. A critical determination to be made is whether the water temperature can be explained by deep circulation of meteoric water with reasonable geothermal gradients or whether a temperature anomaly (e.g., a magma body) might be present at shallow depths. An assessment of tectonics and heat flow over longer periods can be provided by low-temperature thermochronology of bedrock in fault bounded mountain blocks. Granitic lithologies are ideal for this approach, though any rocks containing apatite and zircon are potential targets. Bedrock which has cooled very rapidly and/or recently would be indicative of tectonically active basins and by analysis of

apatite-zircon pairs it may be possible to understand the timing of changes in exhumation rate or the geothermal gradient. These approaches would be most fruitfully targeted to bedrock at the lowest elevations possible. A similar approach can be applied to basinal strata that are exhumed. Cooling ages which are significantly younger than depositional ages can constrain depth of burial and/or geothermal gradients within sedimentary basins.

*Mining and production of lithium-rich brines*

As noted above, the arid climate that is necessary for the genesis of Li-rich brines in closed basins is also a key to production, because the first step in the extraction of Li is solar evaporation. Brines that are pumped to the surface typically carry 200 to 1,400 ppm Li and ideally have a low Mg/Li ratio (<10) as the geochemical behavior of Mg ions can be similar to Li ions in low-temperature aqueous solution and interfere with the Li purification process. Brines are evaporated in a succession of artificial ponds; in the case of Clayton Valley, Nevada, there are nine ponds with a total area of 16 km$^2$ (Garrett, 2004). In each pond in the chain, brine enters at one end, loses some of its water during the ensuing weeks or months, and is transmitted from the other end into the next pond. Multiple ponds are used in order to separate the various evaporite minerals that crystallize out in sequence, and to compensate for the fact that evaporation rate decreases as TDS increases. The evaporite species depend on the initial brine chemistry: at Clayton Valley, calcite, gypsum, halite, sylvite, and glaserite precipitate out, and at one stage, calcium hydroxide is added to induce precipitation of magnesium, as hydroxide (Garrett, 2004). Depending on climate, it takes a few months to two years to achieve a concentrate that is both enriched in Li (to 5,000 ppm at Clayton Valley) and depleted in other cations. This concentrate is pumped from the last pond to a chemical plant where various end products such as Li carbonate, Li hydroxide, and Li metal are produced. Garrett (2004) described the processes at Clayton Valley and Salar de Atacama in considerable detail.

In most instances, Li-enriched oilfield and geothermal brines do not owe their very existence to present-day climate. Extraction of Li from these brines by solar evaporation is therefore not always an option. In the Salton trough geothermal field, fluids that are pumped to the surface to exploit their heat content also contain elevated Li, Mn, and Zn, which are recovered in a proprietary process not involving solar evaporation (Simbol Materials, 2013). This is also a newly prospective approach for pressurized brines beneath the Rock Springs anticline, Greater Green River basin, Wyoming (University of Wyoming, 2013).

## Summary

Because of the extensive use of Li in industrial and technological applications the demand for this critical element will continue to increase. Continental brines enriched in Li are the most economically recoverable form of Li deposits and account for the source of 75% of current Li production. Therefore, it is imperative to develop an understanding of the genesis of these deposits. We have identified and outlined the six common characteristics of the environments for 18 different basins and their respective brines or salt lakes ranging in Li concentration from 10 to 7000 mg/L. These characteristics are (1) arid climate, (2) closed basin containing a salar (salt crust) or saline lake, (3) associated igneous or geothermal activity (4) tectonically driven subsidence, (5) suitable Li source(s), and (6) ample time to concentrate brine. The relative importance of each of these characteristics has not yet been quantified but these characteristics lay the framework for future studies and exploration for continental Li-rich brines.

## Acknowledgments

The authors would like to thank Rockwood Lithium, Ltd. for their continued support of our research at Clayton Valley, Nevada, and at Salar de Atacama, Chile. Their interest and commitment to helping develop a better understanding of the formation of continental Li brines has greatly enhanced our ability to address this important resource. We also thank the USGS for earlier support of the work at Clayton Valley, Nevada through USGS MRERP award G10AP00056 to L. Munk and C.P. Chamberlain. Melissa Jennings is thanked for her review of the paper as well as Terry Jordan for discussions on the geology of Salar de Atacama, Chile. Constructive reviews from Lisa Stillings and Stephen Kesler improved the quality of this manuscript.

REFERENCES

Albers, J.P., and Stewart, J.H., 1972, Geology and mineral deposits of Esmeralda County, Nevada: Nevada Bureau of Mines and Geology Bulletin, v. 78, 88 p.

Alpers, C.N., and Whittemore, D.O., 1990, Hydrogeochemistry and stable isotopes of ground and surface waters from 2 adjacent closed basins, Atacama Desert, northern Chile: Applied Geochemistry, v. 5, p. 719–734.

Arriagada, C., Cobbold, P.R., and Roperch, P., 2006, Salar de Atacama basin: A record of compressional tectonics in the central Andes since the mid-Cretaceous: Tectonics, v. 25, p. 41–44.

Asher-Bolander, S., 1982, Lithium-rich clays, *in* Erickson, R.L. ed., Characteristics of mineral deposit occurrences, U.S. Geological Survey Open-File Report 82-795, p. 225–229.

——1991, Descriptive model of lithium-rich playa brine: U.S. Geological Survey Open-File Report 91-11A, p. 53–54.

Belcher, W.A., ed., 2004, Death Valley regional ground-water flow system, Nevada and California—hydrogeologic framework and transient groundwater flow model: U.S. Geological Survey Scientific Investigations Report 2004-5205.

Benison, K.C., and Bowen, B.B., 2006, Acid saline lake systems give clues about past environments and the search for life on Mars: Icarus, v. 183, p. 225–229.

Bookhagen, B., and Strecker, M.R., 2008, Orographic barriers, high-resolution TRMM rainfall, and relief variations along the eastern Andes: Geophysical Research Letters, v. 35, p. 1–6.

Boschetti, T., Cortecci, G., Barbieri, M., and Mussi, M., 2007, New and past geochemical data on fresh to brine waters of the Salar de Atacama and Andean altiplano, northern Chile: Geofluids, v. 7, p. 33–50.

Bowen, B.B., and Benison, K.C., 2009, Geochemical characteristics of naturally acid and alkaline saline lakes in southern Western Australia: Journal of Applied Geochemistry, v. 24, p. 268–284.

Bradley, D., Munk, L., Jochens, H., Hynek, S., and Labay, K., 2013, A preliminary deposit model for lithium brines: U.S. Geological Survey Open-File Report: 2013-1006, 6 p.

Caine, J.S., Evans, J.P., and Forster, C.B., 1996, Fault zone architecture and permeability structure: Geology, v. 24, p. 1025–1028.

Carmona, V., Pueyo, J.J., Taberner, C., Chong, G., and Thirlwall, M., 2000, Solute inputs in the Salar de Atacama (N. Chile): Journal of Geochemical Exploration, v. 69, p. 449–452.

Collins, A.G., 1976, Lithium abundances in oil field waters, *in* Vine, J.D., ed., Lithium resources and requirements by the year 2000: Geological Society of America, p. 116–122.

Davis, J.R., and Vine, J.D., 1979, Stratigraphic and tectonic setting of the lithium brine field, Clayton Valley, Nevada: Basin and Range Symposium and Great Basin Field Conference, p. 421–430.
Davis, J.R., Friedman, I., and Gleason, J.D., 1986, Origin of the lithium-rich brine, Clayton Valley, Nevada, US: U.S. Geological Survey Bulletin 1622, p. 131–138.
Dresel, P.E., and Rose, A.W., 2010, Chemistry and Origin of Oil And Gas Well Brines in Western Pennsylvania: Pennsylvania Geological Survey Open-File Oil and Gas Report 10-01.0, 48 p.
Eugster, H.P., 1980, Geochemistry of evaporitic lacustrine deposits: Annual Reviews in Earth and Planetary Science, v. 8, p. 35–63.
Eugster, H.P., and Hardie, L.A., 1978, Saline lakes: Springer, New York.
Eugster, H.P., and Jones, B.F., 1979, Behavior of major solutes during closed-basin brine evolution: American Journal of Science, v. 279, p. 609–631.
Evans, K., 2010, The lithium-brine reserve conundrum: Northern Miner, v. 96, p. 2–6.
Flint, S., Turner, P., Jolley, E.J., and Hartley, A.J., 1993, Extensional tectonics in convergent margin basins: An example from the Salar de Atacama, Chilean Andes: Geological Society of America Bulletin 105, p. 603–617.
Garrett, D.E., 2004, Handbook of lithium and natural calcium chloride: Their deposits, processing, uses and properties: Elsevier, 476 p.
Godfrey, L.V., Chan, L.H., Alonso, R.N., Lowenstein, T.K., McDonough, W.F., Houston, J., Li, J., Bobst, A., and Jordan, T.E., 2013, The role of climate in the accumulation of lithium-rich brine in the Central Andes: Journal of Applied Geochemistry, v. 38, p. 92–102.
Gruber, P.W., Medina, P.A., Keoleian, G.A., Kesler, S.E., Everson, M.P., and Wallington, T.J., 2011, Global lithium availability a constraint for electric vehicles?: Journal of Industrial Ecology, v. 15, p. 760–775.
Hacini, M., Kherici, N., and Oelkers, E.H., 2008, Mineral precipitation rates during the complete evaporation of the Merouane Chott ephemeral lake: Geochimica et Cosmochimica Acta, v. 72, p. 1583–1597.
Hardie, L.A., and Eugster, H.P., 1970, The evolution of closed-basin brines: Mineralogical Society of America Special Paper, v. 3, p. 273–290.
Hofstra, A.H., Todorov, T.I., Mercer, C.N., Adams, D.T., and Marsh, E.E., 2013, Silicate melt inclusion evidence for extreme pre-eruptive enrichment and post-eruptive depletion of lithium in silicic volcanic rocks of the Western United States: Implications for the origin of lithium-rich brines: Economic Geology, v. 108, p. 1691–1701.
Hoke, G.D., and Garzione, C.N., 2008, Paleosurfaces, paleoelevation, and the mechanisms for the late Miocene topographic development of the Altiplano plateau: Earth and Planetary Science Letters, v. 271, p. 192–201.
Houston, J., Butcher, A., Ehren, P., Evans, K., and Godfrey, L., 2011, The evaluation of brine prospects and the requirement for modifications to filing standards: Economic Geology, v. 106, p. 1225–1239.
Ide, F., and Kunasz, I.A., 1989, Origin of lithium in Salar de Atacama, northern Chile: Geology of the Andes and its relation to hydrocarbon and mineral resources: Circum-Pacific Council for Energy and Mineral Resources Earth Science Series, Houston, Texas, Proceedings, p. 165–172.
Jochens, H., and Munk, L.A., 2011, Experimental weathering of lithium-bearing source rocks, Clayton Valley, Nevada, USA: Biennial Meeting SGA 2011, 11th, Antofagasta, Chile, Proceedings, p. 238–240.
Jordan, T.E., Godfrey, L.V., Muñoz, N., Alonso, R.N., Lowenstein, T.L., Hoke, G., Peranginangin, N., Isacks, B.L., and Cathles, L., 2002a, Orogenic-scale ground water circulation in the Central Andes: Evidence and consequences: International Symposium on Andean Geodynamics (ISAG), 5th, Toulouse, France, Institut de Recherche Pour le Développement, and Université Paul Sabatier, Proceedings, p. 331–334.
Jordan, T.E., Munoz, N., Hein, M., Lowenstein, T., Godfrey, L., and Yu, J., 2002b, Active faulting and folding without topographic expression in an evaporite basin, Chile: Geological Society of America Bulletin v. 114, p. 1406–1421.
Jordan, T.E., Mpodozis, C., Munoz, N., Blanco, N., Pananont, P., and Gardeweg, M., 2007, Cenozoic subsurface stratigraphy and structure of the Salar de Atacama basin, northern Chile: Journal of South American Earth Sciences, v. 23, p. 122–146.
Jordan, T.E., Nester, P.L., Blanco, N., Hoke, G.D., Davila, F., and Tomlinson, A.J., 2010, Uplift of the Altiplano-Puna plateau: A view from the west: Tectonics v. 29, TC5007, doi:10.1029/2010TC002661.
Kampf, S.K., Tyler, S.W., Ortiz, C.A., Muñoz, J.F., and Adkins, P.L., 2005, Evaporation and land surface energy budget at the Salar de Atacama, northern Chile: Journal of Hydrology, v. 310, p. 236–252.
Kesler, S.E., Gruber, P.W., Medina, P.A., Keoleian, G.A., Everson, M.P., and Wallington, T.J., 2012, Global lithium resources: Relative importance of pegmatite, brine and other deposits: Ore Geology Reviews, v. 48, p. 55–69.
Kuhn, D., 2002, Fold and thrust belt structures and strike-slip faulting at the SE margin of the Salar de Atacama basin, Chilean Andes: Tectonics, v. 21, 1026, doi:10.1029/2001TC901042.
Kunasz, I.A., 1974, Lithium occurrence in the brines of Clayton Valley, Esmeralda County, Nevada: Symposium on Salt, 4th, Northern Ohio Geological Survey, Proceedings, p. 57–66.
Lindsay, J.M., Schmitt, A.K., Trumbull, R.B., De Silva, S.L., Siebel, W., and Emmermann, R., 2001, Magmatic evolution of the La Pacana caldera system, Central Andes, Chile: Compositional variation of two cogenetic, large-volume felsic ignimbrites: Journal of Petrology v. 42, p. 459–486.
Mohr, S., Mudd, G., and Giurco, D., 2010, Lithium resources and production: A critical global assessment: Prepared for CSIRO Minerals Down Under Flagship, by the Institute for Sustainable Futures (University of Technology, Sydney) and Department of Civil Engineering (Monash University), 99 p.
Moraga, A., Chong, G., Fortt, M.A., and Henriquez, H., 1974, Estudio geolo´gico del salar de Atacama, Provincia de Antofagasta: Santiago, Chile, Boletin Instituto de Investigaciones Geológicas, v. 29, p. 1–56.
Mpodozis, C., Arriagada, C., Basso, M., Roperch, P., Cobbold, P., and Reich, M., 2005, Late Mesozoic to Paleogene stratigraphy of the Salar de Atacama Basin, Antofagasta, Northern Chile: Implications for the tectonic evolution of the Central Andes: Tectonophysics, v. 399, p. 125–154.
Munk, L., Jennings, M., Bradley, D., Hynek, S., Godfrey, L., and Jochens, H., 2011, Geochemistry of lithium-rich brines in Clayton Valley, Nevada, USA: Biennial Meeting SGA 2011, 11th, Antofagasta, Chile, Proceedings, p. 211–213.
Oldow, J.S., Bally, A.W., Avé Lallemant, H.G., and Leeman, W.P., 1989, Phanerozoic evolution of the North American cordillera, United States and Canada, Bally, A.W., and Palmer, A.R., eds., The Geology of North America-Vol. A. An Overview: Geological Society of America, p. 139–232.
Pananont, P., Mpodozis, C., Blanco, N., Jordan, T.E., and Brown, L.D., 2004, Cenozoic evolution of the northwestern Salar de Atacama basin, northern Chile: Tectonics, v. 23, TC6007, doi:10.1029/2003TC001595.
Placzek, C.J., Quade, J., and Patchett, P.J., 2011, Isotopic tracers of paleohydrologic change in large lakes of the Bolivian Altiplano: Quaternary Research, v. 75, p. 231–244.
Price, J.G., Lechler, P.J., Lear, M.B., and Giles, T.F., 2000, Possible volcanic sources of lithium in brines in Clayton Valley, Nevada: Geology and Ore Deposits 2000: The Great Basin and Beyond, Geological Society of Nevada, Proceedings, p. 241–248.
Rettig, S.L., Jones, B.F., and Risacher, F., 1980, Geochemical evolution of brines in the Salar of Uyuni, Bolivia: Chemical Geology, v. 30, p. 57–79.
Risacher, F., and Fritz, B. G., 1991, Geochemistry of Bolivian Salars, Lipez, southern Altiplano—origin of solutes and brine evolution: Geochimica et Cosmochimica Acta, v. 55, p. 687–705.
——2009, Origin of salts and brine evolution of Bolivian and Chilean salars: Aquatic Geochemistry, v. 15, p. 123–157.
Risacher, F., Alonso, H., and, Salazar, C., 1999, Geoquímica de aguas en cuencas cerradas, I, II, III Regiones, Chile: Santiago, Chile, Series de Informes Tecnicos Ministerio de Obras Públicas, Dirección General de Aguas, Technical Report.
——2003, The origin of brines and salts in Chilean salars: A hydrochemical review: Earth-Science Reviews, v. 63, p. 249–293.
Robinson, P.T., 1972, Petrology of the potassic Silver Peak volcanic center, western Nevada: Geological Society of America Bulletin, v. 83, p. 1693–1708.
Rush, F.E., 1968, Index of hydrographic areas in Nevada: Nevada Division of Water Resources Information Report 6, 38 p.
Salisbury, M.J., Jicha, B.R., de Silva, S.L., Singer, B.S., Jimenez, N.C., and Ort, M.H., 2011, $Ar^{40}/Ar^{39}$ chronostratigraphy of Altiplano-Puna volcanic complex ignimbrites reveals the development of a major magmatic province: Geological Society of America Bulletin, v. 123, p. 821–840.
Sarna-Wojcicki, A.M., Reheis, M.C., Pringle, M.S., Fleck, R.J., Burbank, D., Meyer, C.E., Slate, J.L., Wan, E., Budahn, J.R., Troxel, B., and Walker, J.P., 2005, Tephra layers of blind Spring Valley and related upper Pliocene and Pleistocene tephra layers, California, Nevada, and Utah: Isotopic ages, correlation, and magnetostratigraphy: U.S. Geological Survey Professional Paper 1701, 63 p.
Schmitt, A.K., 2001, Gas-saturated crystallization and degassing in large-volume, crystal-rich dacitic magmas from the Altiplano-Puna, northern Chile: Journal of Geophysical Research-Solid Earth, v. 106, p. 30,561–30,578.

Schurr, B., and Rietbrock, A., 2004, Deep seismic structure of the Atacama basin, northern Chile: Geophysical Research Letters v. 31, L12601, doi:10.1029/2004GL019796.

Simbol Materials, 2013, http://www.simbolmaterials.com/breakthrough_technology.htm

Spiro, B., and Chong, G., 1996, Origin of sulfate in the Salar de Atacama and the Cordillera de la Sal, initial results of an isotopic study: International Symposium on Andean Geodynamics, 3rd, Paris, Saint Malo, France, Orstom Editions, Collection Colloques et Seminaires, p. 703–705.

Strecker, M.R., Alonso, R.N., Bookhagen, B., Carrapa, B., Hilley, G.E., Sobel, E.R., and, Trauth, M.H., 2007, Tectonics and climate of the southern central Andes: Annual Review of Earth and Planetary Sciences, v. 35, p. 747–787.

Tahil, W., 2008, The trouble with lithium 2: Under the microscope: Martainville, France, Meridian International Research.

Toledo, A.O., Alonso, R.N., V. Ruiz, T., and Quiroga, A.G., 2009, Evapofacies Halítica en el Salar del Rincón, Departamento Los Andes, Salta: Revista de la Asociación Geológica Argentina, v. 64, p. 493–500.

University of Wyoming, 2013, UW researchers' lithium discovery could boost $CO_2$ storage prospects: (http://www.uwyo.edu/uw/news/2013/04/uw-researchers-lithium-discovery-could-boost-co2-storageprospects.html).

U.S. Geological Survey, 2011, Mineral commodity summaries 2011: Lithium.

Vine, J.D., 1980, Where in the world is all the lithium? U.S. Geological Survey Open-File Report 80-1234, 107 p.

Warren, J.K., 2010, Evaporites through time: Tectonic, climatic and eustatic controls in marine and nonmarine deposits: Earth-Science Reviews v. 98, p. 217–268.

Yaksic, A., and, Tilton, J.E., 2009. Using the cumulative availability curve to assess the threat of mineral depletion: The case of lithium: Resources Policy v. 34, p. 185–194.

Yu, J., Gao, C., Cheng, A., Liu, Y., Zhang, L., and, He, X., 2013, Geomorphic, hydroclimatic and hydrothermal controls on the formation of lithium brine deposits in the Qaidam basin, northern Tibetan plateau, China: Ore Geology Reviews, v. 50, p. 171–183.

Zampirro, D., 2004, Hydrogeology of Clayton Valley brine deposits, Esmeralda County, Nevada: Forum on the Geology of Industrial Minerals, 39th, Reno, Nevada, Proceedings.

# APPENDIX

## Summary

This Appendix provides detailed information on the geology and tectonics of each basin listed in Table 1 of the main paper. References for other information included in Table 1 are also detailed here. Table S1 at the end of this Appendix contains various geochemical data for hot springs, thermal water, and nonthermal water in some Li-rich brine-bearing basins. This data, collected by the authors, augment Table 1 and the Appendix text.

## Middle East

The Dead Sea is the only saline water considered from the Middle East. Importantly, this saline water has developed in extremely arid conditions. It is surrounded by the eastern Mediterranean, the Horn of Africa, and the Arabian Peninsula—three of the most arid regions on the planet.

### *Dead Sea*

The Dead Sea is not part of the world ocean but rather is a terminal salt lake. The lake is the most saline in the world (>30% dissolved solids; Garfunkel and Ben-Avraham, 1996), and the basin contains the topographically lowest dry land. The Dead Sea occupies an intracontinental pull-apart basin along the sinistral transform boundary between the Arabian and African plates (Garfunkel and Ben-Avraham, 1996). Recent drawdown of the Dead Sea, which is due to agricultural overuse of surface water from the River Jordan, has resulted in the separation of lake water into northern and southern lakes. The southern lake is largely divided into evaporating ponds where potash and bromide are produced (Garrett, 2004). The end liquor reportedly has subeconomic Li concentrations of 30 mg/L (Garrett, 2004). The shores of the southern lake are dotted with hot springs. In a synthesis of evidence for active faulting in along this plate boundary zone, Garfunkel et al. (1981) noted that a late Pliocene to early Pleistocene basaltic unit (cover basalt) is widely distributed.

Notes for Table 1: Average Li concentration from Garrett (2004). Garrett (2004) also estimated 2 Mt of Li resource in the Dead Sea, although it is not identified as a major source of Li to date because the concentration of Li is quite low.

## North American Basins Containing Li Brines

### *Salton trough, California*

The Salton trough is a strike-slip basin located at a releasing bend along an intracontinental segment of the San Andreas transform fault (Axen and Fletcher, 1998). Looking to the south, the San Andreas fault is seen to be the northernmost of a series of transforms that connect short ridge segments across which the Gulf of California has opened by seafloor spreading in the past few million years. The Salton trough, then, is akin to one of the ridge segments, a key difference being that extension has not yet reached the stage of seafloor spreading. The lithium-enriched brines in the Salton trough are geothermal fluids at 100° to 300°C (Garrett, 2004, p. 37) that are produced from young basin-fill strata in the transtensional basin. The Colorado River was probably a major sediment source (Winker and Kidwell, 1986). Robinson et al. (1976) reported that sediments of the Colorado River delta are intruded by Quaternary rhyolite domes. The lithium resource has been known for decades but only recently did production start, by Simbol, Inc., as a byproduct of geothermal energy production(http://www.simbolmaterials.com/breakthrough_technology.htm).

Notes for Table 1: All reported Li values from Garrett (2004). Total Li resource from Gruber et al. (2011).

### *Searles Lake, California*

Searles Valley is a Neogene basin within the broad intersection between the E-striking, sinistral Garlock fault system and the eastern California shear zone of Dokka and Travis (1990), a N-striking zone of diffuse dextral shear. Extension appears to be the main driver of subsidence. A normal fault system marked by a pronounced surface graben follows the basin's eastern edge at the foot of the Slate Range (Smith, 2009). The Garlock fault, near the southern limit of the basin, is active, as revealed by a Quaternary sinistral offset of about 90 m (McGill and Sieh, 1993). During relatively wet intervals in the past few million years, Searles Lake was the third in a chain of five lakes on the east side of the Sierra Nevada Mountains, the lowest and final one being Death Valley (Smith, 2009). The spillways, through which each of the first four paleolakes drained to the next one, are now far above the present lake or playa surfaces. Searles Valley does not appear to be prospective for geothermal resources; however, the Coso geothermal field lies within the next basin upstream (China Lake; Smith, 1976). Quaternary tufa pinnacles of lacustrine origin are inferred to line up along buried faults (Smith, 2009). Mafic lavas as young as 1.75 Ma crop out nearby. The Lava Creek ash (0.64 Ma) has been identified in the basin fill (Izett and Wilcox, 1982). Curiously, some brines and muds in Searles Valley are enriched in tungsten (Ririe, 1989).

Notes for Table 1: Minimum, maximum, and average Li concentrations from Garrett (2004), the average is from the middle part of the lake.

### *Great Salt Lake, Utah*

The geology of Great Salt Lake is dominated by Paleozoic marine strata exposed in horsts of the Basin and Range extensional province. Great Salt Lake is bordered on the east by the Wasatch Mountains, the largest and most continuous fault-bounded mountain block in the eastern Basin and Range. The Wasatch Mountains define the edge of Basin and Range extension in northern Utah, and by virtue of their abundant snowpack they provide a major source of water to Great Salt Lake. However, the three major freshwater sources for Great Salt Lake, the Provo/Jordan River system, the Weber River, and the Bear River, all drain the quartzite-dominated Neoproterozoic Uinta Mountain Group in the western Uinta Mountains before traversing the Wasatch Mountains. The Wasatch and adjacent Oquirrh Mountains are intruded by granodiorite and quartz monzonite intrusions, which precede and coincide with an Oligocene and early Miocene ignimbrite flareup in the Basin and Range (Best et al., 2013). This ignimbrite flareup has drawn comparison with the Mio-Pliocene Central Andean flareup, and it is likely that crustal thickness in the

Basin and Range at this time was similar to the present-day Andean Plateau (Best et al., 2009). The 36 to 18 Ma flareup is related to a variety of metal deposits of economic importance, including Marysvale volcanic field in central Utah. In the Oquirrh Mountains, immediately south of Great Salt Lake the Bingham Canyon mine exploits a large porphyry copper deposit related to this event. During paleoclimatic intervals where lake levels were higher, the Great Salt Lake subbasin has also been connected to the Sevier subbasin, which contains younger volcanic rocks. These young volcanic rocks are much more interesting from a Li source perspective. They contain basaltic flows and tuff cones (Pushkar and Condie, 1973)—some of which were subaqueous eruptions in Lake Bonneville (White, 1996), and topaz rhyolites that contain extraordinary enrichments in Rb, Cs, Li, and Be (Congdon and Nash, 1988) and host the important volcanogenic beryllium deposit at Spor Mountain, Utah (Foley et al., 2010).

Great Salt Lake is the remnant of the glacial Lake Bonneville, whose climatically driven lake-level record is well known for the last 30 ka (Oviatt, 1997). The late Quaternary Bonneville highstand (pre 17.5 ka) was contemporaneous with maximum glaciation in the Wasatch Mountains, which began its retreat at ~16 ka (Laabs et al., 2011). A longer term history of lake-level fluctuations in the Bonneville basin is known to extend back at least 750 ka and is broadly correlated with extensive Northern Hemisphere glactiation (Oviatt et al., 1999). It is believed that rapid desiccation of deep freshwater lakes led to deposition of thick evaporite units (Balch et al., 2005).

Two important aspects of the late Quaternary and modern hydrology of the Bonneville basin and Great Salt Lake are salient to sources of Li and concentration of Li in Great Salt Lake and Sevier Lake (in the Sevier subbasin). The first (paleo)hydrologic point of interest is the geomorphic threshold that separates the two subbasins at the Old River Bed, near Table Mountain, Utah. At ~14,500 ka Lake Bonneville fell below the threshold that separates the Sevier subbasin from the Great Salt Lake subbasin; from this point until ~11,500 ka Lake Gunnison occupied the Sevier subbasin and overflowed into the Great Salt Lake subbasin (Oviatt et al., 2003). Lake Gunnison was fed by the Beaver and Sevier Rivers originating in the Tushar Mountains (Marysvale volcanic field); this drainage is assumed to be the same as modern and freshwater inputs dominated by the Sevier River. Since ~11,500 ka the Sevier River has been the major source of freshwater to Sevier Lake, though in recent times irrigation has effectively reduced this input to zero. A subsurface brine exists within a meter of the land surface underneath Sevier Lake playa. This Na-Cl brine contains ~30 mg/L lithium and appears to be perched in the upper 10 m of Sevier Lake above fresher water (Whelan, 1969). Almost nothing is known about groundwater flux to the basin, but presumably the Sevier Lake brine is perched on lacustrine clays related to Lake Bonneville and Lake Gunnison. Consequently, it can be assumed that the lithium in this brine has been concentrated over the Holocene. A number of interesting thermal springs exist in the region, including Baker Hot Springs ~60 km north of Sevier Lake, but within the drainage basin, and the Roosevelt Known Geothermal Resource Area (KGRA) at the southeastern margin of the drainage basin. However, the Sevier River likely provided the vast majority of the influx over this period and may be the major source of Li to the Sevier Lake basin.

The second (paleo)hydrologic point of interest is the potential Quaternary diversions of the Bear River into and out of the Great Salt Lake subbasin. At present the Bear River is one of the three major sources of freshwater to Great Salt Lake, though at different points in the late Quaternary it may have been diverted into and out of the Bonneville (Great Salt Lake) basin repeatedly (Bouchard et al., 1998). The input of the Bear River is important from the perspective of the Sr isotope hydrology and paleohydrology of Great Salt Lake (Jones and Faure, 1972; Hart et al., 2004). In fact, the Bear River dominates the Sr isotope hydrology not only because of its high discharge, but also because of its high Sr concentrations owing to contributions from Crystal Hot Springs. Influx from Crystal Hot Springs changes the composition of the Bear River, and adds substantial Li. Our samples from hot and cold springs in this region contain 1.8 to 6.5 mg/L Li (cf. Table S1) and presumably this is the major Li source for Great Salt Lake. Analyses from the 1960s (Handy, 1967; Whelan, 1969) converge on Li concentrations in the range of 40 to 70 mg/L, though more recent analyses report Li concentrations <30 mg/L (Jones et al., 2009).

Although Li is not economical to extract from Great Salt Lake, the minerals industry is very active in Great Salt Lake—as of 2005, six mining companies extracted dissolved and solid components from the lake, including common salts, potassium sulfate, magnesium chloride, magnesium (metal), chloride (gas), sodium sulfate, and calcium sulfate (http://www.deq.utah.gov/workgroups/gsl_wqsc/docs/2005/Mar/GSLChemistry.pdf).

Notes for Table 1: Minimum, maximum, average Li concentration and total Li resource from Garrett (2004). Li concentration of nearby hot springs and associated surface water from S. Hynek (this paper).

### *Clayton Valley, Nevada*

A good overview of the geology and physiography of Clayton Valley can be found in Kunasz (1974). Clayton Valley is an extensional basin with a valley floor occupied by a 20-km$^2$ playa (Kunasz, 1974). It is located in the Basin and Range province, the world's widest hyperextended terrain. Extension in the Basin and Range province, in turn, has taken place above an asthenospheric slab window along a former convergent margin, the extension being the consequence of complex ridge-trench-transform interactions (Dickinson and Snyder, 1979). Deformation in this part of the Basin and Range province is relatively young (mid-Miocene to Pliocene) and related to transtension within the broad structure known as Walker Lane (Oldow et al., 2009). In detail, Clayton Valley is hosted in an extensional half-graben system between a young metamorphic core complex to the west (Mineral Ridge Core Complex: Oldow et al., 2009) and its breakaway zone to the east (Montezuma Range). Low-angle extension has pulled the rocks of the core complex up from their original position at depth; this process has juxtaposed the basin fill against hot rocks. Before the groundwater system was disrupted by lithium brine production, hot springs were located at the eastern and western basin margins (Davis and Vine, 1979). The basin is being evaluated for geothermal resources (Anonymous, 2012). A well-formed

basaltic cinder cone is located within a few kilometers of the brine field; this volcano is undated but probably Quaternary in age. The basin fill sequence includes many horizons of glassy, felsic tuff from a variety of local and distant Neogene eruptive centers, including the Bishop tuff (Sarna-Wojcicki et al., 2000) that blanketed much of the Basin and Range and which constitutes an important Li-rich brine aquifer in the Clayton Valley brine field (Zampirro, 2004). Price et al. (2000) reported Li concentrations as high as 228 ppm in silicic tuffs within the Clayton Valley drainage area.

Notes for Table 1: Average Li concentration is from Harben and Edwards (1998) and the minimum and maximum Li concentrations are from Garrett (2004). Lithium in nearby hotsprings from Davis et al. (1986). Lithium resource estimate from Gruber et al. (2011).

## Evaporite Basins (Salars) of the Central Andes

The Central Andes of South America host the largest and most numerous Li brine deposits in the world. Two important physiographic features if the Central Andes figure prominently in the generation of Li brines; the Central Andean plateau and the Atacama Desert. In these environments, the combination of volcanism, hydrothermal activity, closed basins, and hyperarid climate has led to extensive deposition of evaporite deposits since ~15 Ma (Alonso et al., 1991). The extreme size and longevity of these closed basins is very favorable for generation of Li brines, particularly where thick evaporite deposits (halite, gypsum, and less commonly borates) have removed ions from solution, further concentrating Li. A general overview of the geology and mineral resources of Central Andean salars can be found in Ericksen et al. (1990).

The Central Andean plateau is the world's second largest and highest orogenic plateau; only the Tibetan plateau is higher or more extensive (Allmendinger et al., 1997; Strecker et al., 2007). This high-altitude plateau is a hydrographically closed topographic feature in the back arc of the Neogene Andes. A series of closed basins at tropical and subtropical southern latitudes comprise the Central Andean plateau. Although the full extent of the plateau includes Bolivia, northwestern Argentina, and portions of Chile and Peru, the salars of interest belong to three main groups; those of the Bolivian Altiplano, those of the Argentine Puna, and those of the Chilean Atacama Desert at the western margin of the plateau. The Altiplano of Bolivia has more subdued reflief and is dominated by the extremely large Salar de Uyuni and its satellite salar, Copaisa. Additionally, Salar de Pastos Grandes is a smaller closed basin within the Uyuni hydrographic basin, which sits at a higher elevation (~4,450 m) than Uyuni and Copaisa (~3,650 m). The salars in the Argentine portion of the plateau share more characteristics with the Bolivian Salar de Pastos Grandes (not to be confused with the Argentine Salar de Pastos Grandes) than they do with the giant Uyuni/Copaisa system. These salars on the Argentine Puna plateau have much smaller surface areas and typically their hydrographic boundaries are defined by some combination of volcanic edifices, crystalline mountain blocks, and alluvial deposits. The Chilean salars discussed span the latitudinal range of the Atacama Desert (18°–27° S); at the northern and southern ends, the Salars de Surire and Maricunga, respectively, lie at the western margin of the Puna-Altiplano plateau with elevations exceeding 4,000 m. In the central Atacama, the giant Salar de Atacama lies on the Tropic of Capricorn at 2,300-m elevation.

### *Salars of the Altiplano plateau*

Salars on the Altiplano plateau discussed herein are (from north to south) Copaisa, Uyuni, and Pastos Grandes. These salars occupy the same hydrographic basin and contain a rich record of climatically driven lake-level history. The Andean volcanic arc defines the western margin of the Altiplano. The topography on the Altiplano is generally subdued relative to the southern portion of the Central Andean plateau and recent volcanic activity is also less abundant. The Li resources in the Bolivian Altiplano are substantial, but the Mg/Li ratio of these brines is not favorable for Li production using current technology.

*Salar de Copaisa:* This is a satellite lake to Uyuni; they were connected during periods of higher lake level. This connection occurred as recently as the latest Quaternary or early Holocene. A thorough discussion of lake-level histories and the connections between basins can be found in Plazcek et al. (2006, 2011). Modern Salar de Copaisa is fed by drainages from the north.

Notes for Table 1: Average Li concentration from Garrett (2004).

*Salar de Uyuni:* Salar de Uyuni is the remnant of a large glacial lake, and the world's largest salt flat. The climatic history of the region from ~120 ka to present is documented by paleolake shores in the Uyuni, and adjacent Poopo and Coipasa basins (Plazcek et al., 2006). Modern Salar de Uyuni is fed by the Río Grande de Lipez from the south; this drainage area includes young rhyolites.

Notes for Table 1: Lithium concentrations from Garrett (2004) and total Li resource from Gruber et al. (2011).

*Salar de Pastos Grandes*: Altiplano plateau, southeastern Bolivia. The Salar de Pastos Grandes occupies a small portion of the ~60- × 35-km oval collapse caldera first identified by Baker (1981), using satellite imagery. This caldera presumably formed during eruption of the 5.45 Ma Chuhuilla Ignimbrite and was last active during eruption of the 2.89 Ma Pastos Grandes Ignimbrite which erupted ~1,500 $km^3$ of Dense Rock Equivalent (DRE) material (Salisbury et al., 2011). The Pastos Grandes caldera is the northernmost caldera in the Altiplano-Puna volcanic complex, and the Pastos Grandes Ignimbrite formed during the youngest documented supereruption in the complex. Currently, the Salar de Pastos Grandes is bordered to the south and the west by resurgent lava domes; whereas the northern and eastern boundaries of the salar are the caldera scarp. With respect to generation of the lithium brine at Pastos Grandes, de Silva and Francis (1991) made two relevant observations: (1) in addition to Pastos Grandes, several other lakes "may be remnants of a much more extensive lake which once occupied much of the moat of Pastos Grandes caldera," and (2) "Of several hot springs associated with the caldera, the largest is in the Laguna Pastos Grandes. These provide evidence for continuing geothermal activity within the underlying plutonic system."

Notes for Table 1: Lithium concentrations from Lando (2010).

*Salars of the Puna plateau*

The Puna plateau is the southern portion of the high elevation internally drained Central Andean plateau. The Puna is distinct from the northern portion (Altiplano) of the Central Andean plateau in that it has more youthful topography characterized by basins and ranges; these are often composed of Ordovician bedrock and also exposed Tertiary sediments. Volcanism on the Puna consists of the Andean arc at its western margin and bimodal volcanism in the back arc. Young back-arc mafic rocks are widely distributed throughout the plateau (Kay et al., 1994). Both large and small silicic calderas are also present (de Silva and Francis, 1991; Siebel et al., 2001). Trumbull et al. (2006) conducted a thorough review of the spatiotemporal dynamics of volcanism in both the frontal magmatic arc and the back-arc plateau. More recent work has improved understanding of geochronology and geochemistry of both mafic (Risse et al., 2008) and silicic (Kay et al., 2010) volcanic centers. There are several large, potentially crustal-scale, lineaments or faults that play an important role in the magmatism and fluid flow of the region. These NW-SE-trending lineaments are closely associated with many of the Li-rich salars in the region and have had dynamic interactions with volcanism and individual volcanic centers (Ramelow et al., 2006; Petrinovic et al., 2010). In fact, these lineaments can be considered an important first-order feature in ore deposit models and exploration geology (Chernicoff et al., 2002). The surficial geology of the Puna is dominated by the crustal blocks that constitute the ranges, late Cenozoic sediments and volcanoes, Quaternary alluvium and salar surfaces. The basins commonly contain volcanic, clastic, and evaporite deposits 3 to 5 km thick (Alonso et al., 1991). Internally drained, evaporite depositional centers have existed in the region since ~15 Ma (Vandervoort et al., 1995). Presently, salars are estimated to occupy ~5% of the surface of the Puna plateau, a ~5,000 km$^2$ area (Toledo et al., 2009).

*Salar de Olaroz/Cauchari, Puna plateau, northwestern Argentina:* The Salars de Olaroz and Cauchari are in the same tectonic basin but are separated by alluvial deposits related to the Ola River, which flows into the northern Salar de Cauchari. The southern portion of Salar de Cauchari is fed by the Río Tocomar, originating at the Tocomar volcanic center (see the Salar del Rincón section for further information). Salar de Olaroz is fed from the north by Río El Rosario (also Río El Toro). Little information can be found about springs or thermal waters in the basin, but a study of opaline silica nodules in alluvial fans on the margin of Salar Olaroz concluded that these nodules were indicative of high-silica thermal waters (Bustillo and Alonso, 1989).

There is a history of borate mining in the basin by several companies, and currently two lithium exploration/production companies are active in the basin. It is from their publically available information that most of the data regarding Li concentrations and reserves are derived. A resource evaluation presented for Lithium Americas Corporation in 2010 provides significant data on both Olaroz and Cauchari (http://www.lithiumamericas.com/downloads/Inferred-Resource-Estimate-May_6_2010.pdf; last accessed August 27, 2013). This report details the Li concentrations in surface and subsurface brines, in addition to developing an initial hydrostratigraphic model.

A total of 55 surface brines sampled from hand-dug pits mostly yielded brines containing between 200 and 1,000 mg/L Li. Lithium concentrations in surface brines reached a minimum (<200 mg/L) at the south end of Cauchari and in the boundary zone between Olaroz and Cauchari, and they reached a maximum (>1,000 mg/L) in the central zone of Cauchari. Subsurface brines were evaluated by sampling nine boreholes at 1-m-depth increments; a total of 760 brine samples yielded Li concentrations similar to the mean surface brine value. Three holes in Olaroz yielded average Li concentrations of 347, 456, and 552 mg/L. The weighted mean of all brines sampled from six boreholes in Cauchari is 681 mg/L Li and one of these boreholes yielded an average of 869 mg/L Li ($n$ = 114). These Li concentration data, combined with lithological and hydrological characterization of the basins, were used to arrive at an estimated Li reserve of 0.93 Mt. A subsequent report provides information on additional drilling, geophysical surveys, and hydrologic modeling, but the details of brine volume and lithium concentration changed very little (http://www.lithiumamericas.com/downloads/LAC_NI_43-101_Updated_12062010.pdf; last accessed August 27, 2013). Li reserve estimates of Lithium Americas Corporation combined with estimates (~0.27 Mt Li) put forth by Orocobre Limited for its property on Olaroz (http://www.orocobre.com.au/Projects_Olaroz.htm; last accessed August 27, 2013) put the estimated lithium in this system well over 1 Mt. As of November 2012, Orocobre was developing this property with the aim of producing battery-grade lithium carbonate late in the spring of 2014.

Notes for Table 1: Lithium concentrations in Table 1 from Mohr et al. (2010) and references within and are similar to the values reported by Lithium Americas above. Total Li resource taken from the above estimates.

*Salar del Rincón, Puna plateau, northwestern Argentina:* The Salar del Rincón is a typical Puna basin, delimited by a combination of fault-bounded mountain blocks, stratovolcanoes, and coarse alluvial deposits. To the north, the basin is bound by alluvium and to the east by Sierra de Guayaos, which are composed of Ordovician sedimentary rocks and exposed Tertiary strata. Along its western and southern margins, Salar del Rincón is bound by volcanoes. Less than 50 km west of Salar de Rincón is the Tocomar volcanic center, which is known to have volcanic eruptions within the last 1 Ma and has associated springs and geothermal features associated with the NW-SE-trending,regional-scale Calama-Olacapato-El Toro fault (Petrinovic and Piñol, 2006). The older three volcanic edifices separate this basin from Salar de Pocitos to the south (Cerro Tul-Tul, Cerro del Medio, and Cerro Pocitos) and are also associated with the Calama-Olacapato-El Toro fault zone (Petrinovic et al., 2006). Within the basin, paleohot-spring deposits are identified, and residual water within these deposits was observed to contain as much as 1,500 mg/L of Li (Toledo et al., 2009). Toledo et al. (2009) also presented an assessment of the Li resources in the salar, based upon a drilling program that targeted both solids and brines. They observe an average Li content of 400 mg/L in the brines and present information on the hydrologic characteristics and stratigraphic architecture of the basin. A zone of effective porosity in excess of 30% is identified as well as a zone of lower effective porosity (<10%), together these zones host Li reserves estimated at ~0.2 Mt.

Notes for Table 1: Lithium concentrations in Table 1 from Toledo et al. (2009), as described above.

*Salar de Llullaillaco, Puna plateau, northwestern Argentina:* The Salar de Llullaillaco is located adjacent to a volcano of the same name, which is the world's highest historically active volcano. This lies just outside of the Salar de Atacama surface drainage and due west of the Salar de Arizaro. The Salar de Arizaro, the largest basin preserved within the Puna, contains ~5 km of strata, more than 3 km of them being Miocene lacustrine and eolian deposits (Boyd, 2010). It has been speculated that this basin records delamination of lower crustal material (DeCelles et al., 2011). The potential of lithospheric removal has implications for the generation of lithium-rich brines, as reduced crustal thickness and an influx of hot asthenospheric mantle may play important roles in lithium transport. The potential for lithospheric delamination in an overthickened orogen is supported by geophysical observations, which indicate that the crust is on the order of 42 km thick in this region (Yuan et al., 2002), substantially less thick than predicted based upon the elevation of this region.

Notes for Table 1: Maximum and minimum Li concentrations from Mohr et al. (2010) and references within. Average Li concentration reported in Table 1 is the midpoint of the maximum and minimum.

*Salar del Hombre Muerto, Puna plateau, northwestern Argentina:* Geology in the region of Salar del Muerto is typical of the Puna: Ordovician rocks compose most ranges, basins are filled with late Cenozoic clastic sediments and volcanic rocks, and magmatism is associated with faults in the region (Aceñolaza et al., 1976). The basin containing the Salar del Hombre Muerto is delimited and dissected by faults. Accommodation space within the sedimentary basin was created by Plio-Pleistocene strike-slip deformation (Jordan et al., 1999). Hombre Muerto can be divided into two subbasins and several important differences exist between the two subbasins. Bedrock along the eastern sector of Salar del Hombre Muerto contains metamorphic rocks, which may be some of the oldest rocks in the region (Quenardelle, 1990). The eastern basin also contains borates and has low chloride content, whereas the western basin contains nearly 1 km of halite and almost no borates (Vinante and Alonso, 2006). This is probably related to the surface hydrology of the basin, which is dominated by inflow to the eastern subbasin. These waters drain predominantly young silicic volcanic rocks (Quenardelle, 1987).

In fact, the surface waters that enter the eastern subbasin also drain the interior of one of the world's largest silicic calderas, Cerro Galán. This caldera is an important feature of the southern Puna plateau that was first recognized with spacecraft imagery (Francis et al., 1978, 1983, 1989). An accurate geochronology of the most recent explosive silicic volcanism at Cerro Galan is just emerging (Kay et al., 2011). Based on this data, it is clear that caldera-forming eruptions clustered in a <100-ka interval, the youngest of which is very precisely dated at 2.060 ± 0.004 Ma (Hynek et al., 2011), in close agreement with early Rb-Sr ages (2.03 ± 0.07 Ma; Sparks et al., 1985). These silicic ignimbrites and intracaldera rocks have $^{87}Sr/^{86}Sr$ ratios >0.710 (Sparks et al., 1985; Kay et al., 2011). Thermal water in the region has been observed to have more radiogenic Sr isotope ratios than these ignimbrites (Jordan et al., 1999). This has been interpreted to indicate interaction between thermal waters and radiogenic basement rocks. These data and interpretations are in accord with data we have collected from hot-spring and surface water in the Río Aguas Calientes drainage, which drains the Cerro Galan caldera and feeds the eastern subbasin of the Salar del Hombre Muerto (Table S1). These samples indicate this drainage may be a significant Li source to the salar. A hill slope hot spring discharging into Río Aguas Calientes has an Li content of 5.5 mg/L, and the river into which it flows (Río Aguas Calientes) has an Li content of 3.2 mg/L. Both this hot spring and the river have radiogenic $^{87}Sr/^{86}Sr$ ratios (0.71584 and 0.71763, respectively), considering that these are draining a large silicic volcanic caldera filled with a young rhyodacite ignimbrite.

If the Río Aguas Calientes drainage is the dominant source of Li over the last 2 Ma, its predicted that Li influx must agree with other constraints. Typically it is assumed that halite has been accumulating in the Salar del Hombre Muerto at a rate of ~500 m/Ma for the last 2 Ma (Jordan et al., 1999). This gives a minimum time for generation of the Li brine, which prior to production had between 234 and 1,100 mg/L of Li, with the majority of brines samples containing between 700 to 800 mg/L Li (Nicolli et al., 1982). The climatic history over this interval is less certain, but some constraints do exist. Sediment cores from the Salar del Hombre Muerto indicate that shallow saline lakes have existed in the past, but the region has become progressively drier since ~45 ka (Godfrey et al., 2003).

Notes for Table 1: Maximum, minimum, and average Li concentrations from Garrett (2004). Lithium concentrations of nearby hotsprings from S. Hynek (this paper) and total Li resource from Gruber et al. (2011).

### *Salars of the Atacama Desert*

The Atacama Desert lies in the rain shadow of the hyper-arid Central Andean Plateau. Although the salars of the Atacama are at lower elevations than those of the adjacent plateau, they share many characteristics. Most importantly, salars of the Atacama Desert are intimately associated with volcanism and hydrothermal activity of the Andean magmatic arc. The lacustrine basins of interest all fall between the Cordillera Domeyko and the Altiplano-Puna plateau, a late Quaternary history for many of these basins is provided by Valero-Garcés et al. (2000).

*Salar de Surire, northern Atacama Desert, Chile:* The Salar de Surire is an interesting feature at a high elevation, close to the Altiplano, Volcan Parinacota, and Arica, Chile. Salar de Surire is close to the Uyuni and Coipasa hydrologic basins in Bolivia but is well isolated topographically from them. Geologic studies in a hydrographically closed basin immediately to the north of Salar de Surire provide a relevant tectonic and sedimentary context. The Lauca basin appears to have initiated in the late Miocene and since then has accumulated lacustrine sediments. Plio-Plesitocene evaporite deposits exist and little deformation has occurred since ~6 Ma (Kött et al., 1995).

Notes for Table 1: Average Li concentration and Li concentration of nearby hot springs from Garrett (2004).

*Salar de Atacama, central Atacama Desert, Chile:* The geology of the Salar de Atacama is discussed at length in the text. Here we provide additional information about the older

geologic history. The Cordón de Lila, an anticlinal feature plunging northward into the southern Salar de Atacama, is composed of Paleozoic rocks including marine strata, volcanic successions, and plutonic rocks of predominantly Ordovician age. This block has recently been interpreted to represent a continental magmatic arc at the western margin of Gondwana (Zimmerman et al., 2010). Magmatism along the Gondwanan margin continued into the Late Permian as recorded by volcanic and volcaniclastic strata along the eastern margin of the salar (Breitkreuz, 1995). Thick Permo-Triassic volcanic and continental strata were deposited in the Domeyko basin and are overlain by a Jurassic mixed carbonate/clastic sequence (Flint et al., 1993). These units crop out in the Cordillera Domeyko on the western margin of the salar and are unconformably overlain by Cretaceous and Cenozoic sedimentary rocks associated with the initial uplift of the Cordillera Domeyko and inception of the Salar de Atacama basin (Mpodozis et al., 2005). There was first a foreland basin here, starting in the mid-Cretaceous, with thrusting and coeval sedimentation occurring during the Cretaceous and Paleogene (Arriagada et al., 2006).

Notes for Table 1. Maximum, minimum, and average Li concentrations from Garrett (2004). Lithium concentration of El Tatio hot spring from L.Munk (this paper). Total Li resource estimate from Gruber et al. (2011).

*Salar de Maricunga, southern Atacama Desert, Chile:* The Salar de Maricunga occupies a high elevation intermontane basin between the Cordillera Domeyko and the Andean Cordillera. Salar de Maricunga is situated near the southernmost portion of the Central Andean plateau and also near the southernmost limit of the Atacama Desert. Latorre et al. (2005) remarked that, "With very little rainfall either from tropical or extratropical sources, this sector is undisputedly the driest portion of the Atacama Desert."

Notes for Table 1. The average Li concentration is actually the average Li grade reported by Yaksic and Tilton (2009) and the total Li resource is from Gruber et al. (2011).

## Asian Basins Containing Li Brines

These basins all occur within or on the margins of the Tibetan plateau, therefore, thick orogenic crust is a commonality.

### *Lake Zabuye*

Lake Zabuye is one of a series of high-altitude, terminal lakes in the Shigatse Prefecture of the Tibet Autonomous Region. The Tibetan plateau is the upper plate of the Himalayan-Tibetan collisional orogen, with Tibet comprising the widest and topographically highest orogenic hinterland in the world. Lake Zabuye lies within a Neogene graben that is oriented at high angles to the structural grain of the orogen. The geometry of extension in the basin of Lake Zabuye has not been documented, but 50 km to the west in the Lunggar extensional basin, Woodruff et al. (2013) have shown that extension was asymmetric with the basin having formed above a low-angle, E-dipping detachment. The thrust belt appears to be extending parallel to its strike. The Lake Zabuye area does not appear to have any young volcanic activity or hot springs, although the English-language literature is sparse. A map of Tibetan geothermal resources (Ji, 2008) shows abundant hot springs in many parts of Tibet but none in the Lake Zabuye area. Fourteen elevated strand lines show that Zabuye Lake was once many times larger than today (Yu, 2001). Lake Zabuye has northern and southern arms; the southern one has the brine resource. A notable aspect of this lithium resource is that Lake Zabuye is the only known evaporite system where lithium carbonate precipitates naturally; this is the type locality of the mineral zabuyelite. Wikipedia lists a number of alternate renditions for the name of the lake: Drangyer, Zabayu, Zabuye Caka, Zhabuye, Chabyêr, and Chabyer (http://en.wikipedia.org/wiki/Lake_Zabuye).

Notes for Table 1: Minimum and maximum Li concentrations from Garrett (2004).Average Li concentration and total Li resource from Gruber et al. (2011).

### *Dangxiongcuo (DXC) Lake, Tibet*

English-language information on this Tibetan basin is limited. The most thorough treatment, though far from comprehensive, is from a 2005 vintage industry webpage (essentially, a Powerpoint presentation for investors) by Sterling Group Ventures http://www.sterlinggroupventures.com/Sterling_-_Li_Only_presentation_Sep2005.pdf. The geographic setting and presumably the tectonic origin are similar to those of Lake Zabuye. That is, the lake appears to be in a Neogene graben that is oriented at high angles to the structural grain of the Himalayan-Tibetan collisional orogen. The Sterling Group presentation mentioned hot springs. The name is transliterated as Lake Dangqiongcuo in Google Earth. Transliterated as Damzung Co by Zheng (1997).

Notes for Table 1: Average Li concentration and total Li resource from Gruber et al. (2011).

### *Taijanier Lake, Qaidam, China*

The Qaidam basin is a huge, terminal depocenter in northern Tibet that has subsided since the Paleogene (Yin et al., 2008). On the broadest scale, it can be viewed as an intracontinental foreland basin in the distal, upper-plate hinterland of the Himalayan-Tibetan collisional orogen. The Qaidam basin is bound on the northeast, and loaded by, the Qilian Shan Mountains (Yin et al., 2008). The Qaidam basin is bound by the Kunlun transpressional orogen on the southwest and by the Altyn Tagh strike-slip orogen to the northwest (Yin et al., 2008). Taijanier Lake is one of a number of lakes and salt pans within the greater Qiadam basin. In a series of basin-scale isopach maps, Quaternary sediments are shown as anomalously thick in the area of Taijanier Lake (Yin et al., 2008, fig. 12). Indeed, Taijanier Lake appears to be localized in a growth syncline above a fault-bend fold like those documented and interpreted by Yin et al. (2008) on a nearby basin-scale cross section. An intriguing, newly recognized possibility is that the growth of live folds in the Qaidam basin has been enhanced by wind erosion (Kapp et al., 2011). Boron- and lithium-enriched hydrothermal waters are reported from the Qaidam basin (Zheng M., 1997). A review of the chemistry of lakes in this region is presented by Zheng and Liu (2009).

Notes for Table 1: Average Li concentration from Gruber et al. (2011) and total Li resource from Yaksic and Tilton (2009).

## Table 1: General Information Summary

Topographical and environmental characteristics of the lithium basins were determined through the use of the

Environmental Systems Research Institute (ESRI®) Geographic Information System (GIS) software ArcGIS® Version 10. Several datasets with global coverage were acquired from public sources to provide elevation, drainage, and climatic information. The data included 90-m Shuttle Radar Topograpy Mission (SRTM) Digital Elevation Models (DEMs) from Jarvis et al. (2008), drainage basins from Lehner et al. (2008), temperature and precipitation from Hijmans et al. (2005), and aridity and evapotranspiration from Trabucco and Zomer (2009). The resolutions of the climate datasets were about 1 km.

The outer boundaries and total areas of each closed lithium basin were defined by polygons extracted from the drainage basins dataset. Each of these polygons defined a zone that could be used to extract information from the elevation and climate datasets using statistical tools. The latitude and longitude for a basin were identified by the location of the lowest elevation point within each basin. The area of the basin floor where water could collect was also determined from the elevation data. By isolating a range of elevations, from the minimum elevation up to a threshold value, a section of the topography that matched the maximum extent of the shoreline as shown in satellite imagery could be extracted and its area found. Values for temperature, precipitation, evapotranspiration, and aridity were obtained using zonal statistics to identify the majority value for each parameter in the basins delineated by the drainage polygons.

## NOTES

SRTM 90m Digital Elevation Data: http://srtm.csi.cgiar.org/index.asp

Jarvis, A., H.I. Reuter, A. Nelson, E. Guevara, 2008, Hole-filled SRTM for the globe Version 4, available from the CGIAR-CSI SRTM 90m Database http://srtm.csi.cgiar.org).

Drainage divides: http://hydrosheds.cr.usgs.gov/

Lehner, B., Verdin, K., Jarvis, A. (2008): New global hydrography derived from spaceborne elevation data. Eos, Transactions, AGU, 89(10): 93-94.

Aridity and evapotranspiration: http://csi.cgiar.org/Aridity/

Trabucco, A., and Zomer, R.J. 2009. Global Aridity Index (Global-Aridity) and Global Potential Evapo-Transpiration (Global-PET) Geospatial Database.CGIAR Consortium for Spatial Information. Published online, available from the CGIAR-CSI GeoPortal at: http://www.csi.cgiar.org/

Temperature and precipitation: http://www.worldclim.org/bioclim

Hijmans, R.J., S.E. Cameron, J.L. Parra, P.G. Jones and A. Jarvis, 2005. Very high resolution interpolated climate surfaces for global land areas. International Journal of Climatology 25: 1965–1978.

## REFERENCES


Aceñolaza, F.G., Toselli, A.J., and Gonalez, O., 1976, Geologia de la region comprendida entre el Salar del Hombre Muerto y Antofagasta de la Sierra, Provincia de Catamarca: Revista de la Asociación Geológica Argentina, v. 31, p. 127–136.

Allmendinger, R.W., Jordan, T.E., Kay, S.M., and Isacks, B.L., 1997, The evolution of the Altiplano-Puna plateau of the Central Andes: Annual Review of Earth and Planetary Sciences, v. 25, p. 139–174.

Alonso, R.N., Jordan, T.E., Tabbutt, K.T., and Vandervoort, D.S., 1991, Giant evaporite belts of the Neogene central Andes: Geology, v. 19, p. 401–404.

Anonymous, 2012, Silver Peak area geothermal exploration project environmental assessment DOI-BLM-NV-B020-2012-0214-EA DOE/EA-1921: U.S. Bureau of Land Management, 47 p. [accessed Dec. 26, 2012 at http://www.blm.gov/pgdata/etc/medialib/blm/nv/field_offices/battle_mountain_field/blm_information/nepa/rockwood_silver_peak.Par.86685.File.dat/Rockwood (CFC) Silver Peak Area EA (508 Compliant).pdf].

Arriagada, C., Cobbold, P.R., and Roperch, P., 2006, Salar de Atacama basin: A record of compressional tectonics in the central Andes since the mid-Cretaceous: Tectonics, v. 25, p. TC1008.

Axen, G.J., and Fletcher, J.M., 1998, Late Miocene-Pleistocene extensional faulting, northern Gulf of California, Mexico and Salton trough, California: International Geology Review, v. 40, p. 217–244.

Baker, M.C.W., 1981, The nature and distribution of Upper Cenozoic ignimbrite centers in the central Andes: Journal of Volcanology and Geothermal Research, v. 11, p. 293–315.

Balch, D.P., Cohen, A.S., Schnurrenberger, D.W., Haskell, B.J., Garces, B.L.V., Beck, J.W., Cheng, H., and Edwards, R.L., 2005, Ecosystem and paleohydrological response to Quaternary climate change in the Bonneville basin, Utah: Palaeogeography, Palaeoclimatology, Palaeoecology, v. 221, p. 99–122.

Best, M.G., Barr, D.L., Christiansen, E.H., Gromme, S., Deino, A.L., and Tingey, D.G., 2009, The Great Basin altiplano during the middle Cenozoic ignimbrite flareup: Insights from volcanic rocks: International Geology Review, v. 51, p. 589–633.

Best, M.G., Christiansen, E.H., and Gromme, S., 2013, Introduction: The 36-18 Ma southern Great Basin, USA, ignimbrite province and flareup: Swarms of subduction-related supervolcanoes: Geosphere, v. 9, p. 260–274.

Bouchard, D.P., Kaufman, D.S., Hochberg, A., and Quade, J., 1998, Quaternary history of the Thatcher basin, Idaho, reconstructed from the $^{87}Sr/^{86}Sr$ and amino acid composition of lacustrine fossils: Implications for the diversion of the Bear River into the Bonneville basin: Palaeogeography, Palaeoclimatology, Palaeoecology, v. 141, p. 95–114.

Boyd, J.D., 2010, Tectonic evolution of the Arizaro basin of the Puna plateau, NW Argentina: Implications for plateau-scale processes: M.S. thesis, University of Wyoming, 83 p.

Breitkreuz, C., 1995, The Late Permian Peine and Cas Formations at the eastern margin of the Salar de Atacama, northern Chile: Stratigraphy, volcanic facies, and tectonics: Revista Geológica de Chile, v. 22, 323 p.

Bustillo, M.A., and Alonso, R., 1989, Nodulos Opalinos en Facies Marginales del Salar Olaroz (Puna Argentina): Estudios Geologicos, v. 45, p. 55–59.

Chernicoff, C.J., Richards, J.P., and Zappettini, E.O., 2002, Crustal lineament control on magmatism and mineralization in northwestern Argentina: Geological, geophysical, and remote sensing evidence: Ore Geology Reviews, v. 21, p. 127–155.

Congdon, R.D., and Nash, W.P., 1988, High-fluorine rhyolite: An eruptive pegmatite magma at the Honeycomb Hills, Utah: Geology, v. 16, p. 1018–1021.

Davis, J.R., and Vine, J.D., 1979, Stratigraphic and tectonic setting of the lithium brine field, Clayton Valley, Nevada: RMAG-UGA 1979 Basin and Range Symposium, Proceedings, p. 421–430.

Davis, J.R., Friedman, I., and Gleason, J.D., 1986, Origin of the lithium-rich brine, Clayton Valley, Nevada: U.S. Geological Survey Bulletin 1622, p. 131–138.

DeCelles, P.G., Carrapa, B., Horton, B.K., McNabb, J., and Boyd, J., 2011, Cordilleran hinterland basins as recorders of lithospheric removal in the central Andes [abs.]: American Geophysical Union, Fall Meeting 2011, Abstract T131-06.

de Silva, S.L., and Francis, P.W., 1991, Volcanoes of the central Andes: New York, Springer-Verlag, 216 p.

Dickinson, W.R., and Snyder, W.S., 1979, Geometry of subducted slabs related to San Andreas transform: Journal of Geology, v. 87, p. 609–627.

Dokka, R.K., and Travis, D.J., 1990, Role of the eastern California shear zone in accommodating Pacific-North American plate motion: Geophysical Research Letters, v. 17, p. 323–326.

Ericksen, G.E., Salas O., and Raul, 1990, Geology and resources of salars in the central Andes: Geology of the Andes and its relation to hydrocarbon and mineral resources 11, 151 p.

Flint, S., Turner, P., Jolley, E.J., and Hartley, A.J., 1993, Extensional tectonics in convergent margin basins: An example from the Salar de Atacama, Chilean Andes: Geological Society of America Bulletin, v. 105, p. 603–617.

Foley, N.K., Seal, R.R., Piatak, N.M., and Hetland, B., 2010, An occurrence model for the national assessment of volcanogenic beryllium deposits: U.S. Geological Survey Open-File Report 2010-1195.

Francis, P.W., Hammill, M., Kretzschmar, G.A., and Thorpe, R.S., 1978, The Cerro Galan caldera, north-west Argentina and its tectonic setting: Nature, v. 274, p. 749–751.

Francis, P.W., O'Callaghan, L., Kretzschmar, G.A., Thorpe, R.S., Sparks, R.S.J., Page, R.N., de Barrio, R.E., Gillou, G., and Gonzalez, O.E., 1983, The Cerro Galan ignimbrite: Nature, v. 301, p. 51–53.

Francis, P.W., Sparks, R.S.J., Hawkesworth, C.J., Thorpe, R.S., Pyle, D.M., Tait, S.R., Mantovani, M.S., and McDermott, F., 1989, Petrology and geochemistry of volcanic rocks of the Cerro Galan caldera, northwest Argentina: Geological Magazine, v. 126, p. 515–547.

Garfunkel, Z., and Ben-Avraham, Z., 1996, The structure of the Dead Sea basin: Tectonophysics, v. 266, p. 155–176.
Garfunkel, Z., Zak, I., and Freund, R., 1981, Active faulting in the Dead Sea rift: Tectonophysics, v. 80, p. 1–26.
Garrett, D.E., 2004, Handbook of lithium and natural calcium chloride. Their deposits, processing, uses and properties: Elsevier, 476 p.
Godfrey, L.V., Jordan, T.E., Lowenstein, T.K., and Alonso, R.L., 2003, Stable isotope constraints on the transport of water to the Andes between 22° and 26°S during the last glacial cycle: Palaeogeography, Palaeoclimatology, Palaeoecology, v. 194, p. 299–317.
Gruber, P.W., Medina, P.A., Keoleian, G.A., Kesler, S.E., Everson, M.P., and Wallington, T.J., 2011, Global lithium availability a constraint for electric vehicles?: Journal of Industrial Ecology, v. 15, p. 760–775.
Handy, A.H., 1967, Distinctive brines in Great Salt Lake, Utah: U.S. Geological Survey Professional Paper 575-B, p. B225–B227.
Harben, P., and Edwards, G., 1998, "Lithium: Times are Changing:" Canadian Institue of Mining and Metallurgy Special Volume 50, p. 171–182.
Hart, W.S., Quade, J., Madsen, D.B., Kaufman, D.S., and Oviatt, C.G., 2004, The $^{87}Sr/^{86}Sr$ ratios of lacustrine carbonates and lake-level history of the Bonneville paleolake system: Geological Society of America Bulletin, v. 116, p. 1107–1119.
Hynek, S.A., Brown, F.H., and Fernandez, D.P., 2011, A rapid method for handpicking potassium rich feldspar from silicic tephra: Quaternary Geochronology, v. 6, p. 285–288.
Izett, G.A., and Wilcox, R.E., 1982, Map showing localities and inferred distributions of the Huckleberry Ridge, Mesa Falls, and Lava Creek ash beds (Pearlette family ash beds) of Pliocene and Pleistocene age in the Western United States and Southern Canada: U.S. Geological Survey Miscellaneous Investigation Series Map I-1325, scale 1:4,000,000.
Ji, D., 2008, Geothermal resources and utilization in Tibet and the Himalayas, *in* Fridleifsson, E.B., Workshop for decision makers on direct heating use of geothermal resources in Asia: Iceland: Orkustofnun, 9 p.
Jones, B.F., Naftz, D.L., Spencer, R.J., and Oviatt, C.G., 2009, Geochemical evolution of Great Salt Lake, Utah, USA: Aquatic Geochemistry, v. 15, p. 95–121.
Jones, L.M., and Faure, G., 1972, Strontium isotope geochemistry of Great Salt Lake, Utah: Geological Society of America Bulletin 83, p. 1875–1880.
Jordan, T.E., Alonso, R.N., and Godfrey, L.V., 1999, Tectónica, subsidencia y aguas en el salar del Hombre Muerto, Puna Argentina: Congreso Geológico Argentino, 14th, Actas I, p. 254–256.
Kapp, P., Pelletier, J.D., Rohrmann, A., Heermance, R., and Russell, J., 2011, Wind erosion in the Qaidam basin, central Asia: Implications for tectonics, paleoclimate, and the source of the Loess plateau: GSA Today, v. 21, no. 4/5, doi: 10.1130/GSATG99A.1
Kay, S.M., Coira, B., and Viramonte, J., 1994, Young mafic back arc volcanic rocks as indicators of continental lithospheric delamination beneath the Argentine Puna plateau, central Andes: Journal of Geophysical Research, v. 99, p. 24,323–24,339.
Kay, S.M., Coira, B.L., Caffe, P.J., and Chen, C-H, 2010, Regional chemical diversity, crustal and mantle sources and evolution of central Andean Puna plateau ignimbrites: Journal of Volcanology and Geothermal Research, v. 198, p. 81–111.
Kay, S.M., Coira, B., Worner, G., Kay, R.W., and Singer, B.S., 2011, Geochemical, isotopic and single crystal $^{40}Ar/^{39}Ar$ age constraints on the evolution of the Cerro Galan ignimbrites: Bulletin of Volcanology, v. 73 p. 1487–1511.
Kött, A., Gaupp, R., and Wörner, G., 1995, Miocene to Recent history of the western atiplano in northern Chile revealed by lacustrine sediments of the Lauca basin (18°15'–18°40'S/69°30'–69°05'W): Geologische Rundschau, v. 84, p. 770–780.
Kunasz, I.A., 1974, Lithium occurrence in the brines of Clayton Valley Esmeralda County, Nevada, *in* Coogan, A.H., ed., Fourth International Symposium on Salt, Houston, Tex., April 8–12. 1973, Proceedings: Cleveland, Northern Ohio Geological Society, p. 57–65. (Also available at http://www.saltinstitute.org/content/download/1270/7052).
Laabs, B.J.C., Marchetti, D.W., Munroe, J.S., Refsnider, K.A., Gosse, J.C., Lips, E.W., Becker, R.A., Mickelson, D.M., and Singer, B.S., 2011, Chronology of latest Pleistocene mountain glaciation in the western Wasatch Mountains, Utah, U.S.A.: Quaternary Research, v. 76, p. 272–284.
Lando, J., 2010, Pastos Grandes, lithium brine project, Bolivia: New World Resource Corp. website, http://www.newworldresource.com/s/PastosGrandes.asp (23/07/10).
Latorre, C., Betancourt, J.L., Rech, J.A., Quade, J., Homgren, C., Placzek, C., Maldonado, A., Vuille, M., and Rylander, K.A., 2005, Late Quaternary history of the Atacama Desert *in* Smith, M., and Hesse, P., eds., The archaeology and environmental history of the southern deserts: Canberra, Australia, National Museum of Australia Press, p. 73–90.
McGill, S., and Sieh, K., 1993, Holocene slip rate of the Central Garlock fault in southeastern Searles Valley, California: Journal of Geophysical Research, v. 98, p. 14,217–14,231.
Mohr, S., Mudd, G., and Giurco, D., 2010, Lithium resources and production: A critical global assessment: Prepared for CSIRO Minerals Down Under Flagship, by the Institute for SustainableFutures (University of Technology, Sydney) and Department of Civil Engineering (Monash University), October, 2010, 99 p.
Mpodozis, C., Arriagada, C., Basso, M., Roperch, P., Cobbold, P., and Reich, M., 2005, Late Mesozoic to Paleogenestratigraphy of the Salar de Atacama basin, Antofagasta, northern Chile: Implications for the tectonic evolution of the central Andes: Tectonophysics, v. 399, p. 125–154.
Nicolli, H.B., Surlano, J.M., Méndez, V., and Gómez Peral, M.A., 1982, Salmueras ricas en metales alcalinos del Salar del Hombre Muerto, Provincia de Catamarca, Republica Argentina: Quinto Congreso Lationamericano de Geologia, Argentina, Actas 3, p. 187–204.
Oldow, J.S., Elias, E.A., Ferranti, L., McClelland, W.C., and McIntosh, W.C., 2009, Late Miocene to Pliocene synextensional deposition in fault-bounded basins within the upper plate of the western Silver Peak-Lone Mountain extensional complex, west-central Nevada: Geological Society of America, Special Papers 2009, v. 447, p. 275–312, doi: 10.1130/2009.2447(14). (Also available at http://specialpapers.gsapubs.org/content/447/v.full.pdf+html).
Oviatt, C.G., 1997, Lake Bonneville fluctuations and global climate change: Geology, v. 25, p. 155–158.
Oviatt, C.G., Thompson, R.S., Kaufman, D.S., Bright, J., and Forester, R.M., 1999, Reinterpretation of the Burmester core, Bonneville basin, Utah: Quaternary Research, v. 52, p. 180–184.
Oviatt, C.G., Madsen, D.B., and Schmitt, D.N., 2003, Late Pleistocene and early Holocene rivers and wetlands in western Utah: Quaternary Research, v. 60, p. 200–210.
Petrinovic, I.A., and Piñol, F.C., 2006. Phreatomagmatic and phreatic eruptions in locally extensive settings of southern central Andes: The Tocomar volcanic centre (24°10'S–66°34'W), Argentina: Journal of Volcanology and Geothermal Research, v. 158, p. 37–50.
Petrinovic, I.A., Riller, U., Brrod, J.A., Alvarado, G., and Arnosio, M., 2006, Bimodal volcanism in a tectonic transfer zone: Evidence for tectonically controlled magmatism in the southern central Andes, NW Argentina: Journal of Volcanology and Geothermal Research, v. 152, p. 240–252.
Petrinovic, I.A., Martí, J., Aguirre-Díaz, G.J., Guzmáan, S., Geyer, A., and Salado Paz, N., 2010, The Cerro Aguas Calientes caldera, NW Argentina: An example of a tectonically controlled, polygenetic collapse caldera, and its regional significance: Journal of Volcanology and Geothermal Research, v. 194, p. 15–26.
Placzek, C., Quade, J., and Patchett, P.J., 2006, Geochronology and stratigraphy of late Pleistocene lake cycles on the southern Bolivian altiplano: Implications for causes of tropical climate change: Geological Society of America Bulletin, v. 118, p. 515–532.
——2011, Isotopic tracers of paleohydrologic change in large lakes of the Bolivian altiplano: Quaternary Research, v. 75, p. 231–244.
Price, J.G., Lechler, P.J. et al., 2000, Possible volcanic sources of lithium in brines in Clayton Valley, Nevada: Geology and Ore Deposits 2000: The Great Basin and Beyond Proceedings, v. 1, p. 241–248.
Pushkar, P., and Condie, K.C., 1973, Origin of the Quaternary basalts from the Black Rock Desert region, Utah: Strontium isotopic evidence: Geological Society of America Bulletin, v. 84, p. 1053–1058.
Quenardelle, S.M., 1987, Unidades geomorfologicas en el area del Salar del Hombre Muerto, Puna Argentina, determinadas mediante analisis digital interactivo de imagenes LANDSAT: Decimo Congreso Geologico Argentino, Actas I, p. 365–368.
——1990, Geologia y petrologia del basamento metamorphico del sector oriental del Salar del Hombre Muerto, Puna Argentia: Decimo Primer Congreso Geologico Argentino, Actas I, p. 166–169.
Ramelow, J., Riller, U., Romer, R.L., and Oncken, O., 2006, Kinematic link between episodic trapdoor collapse of the Negra Muerta caldera and motion on the Olacapato-El Toro fault zone, southern central Andes: International Journal of Earth Sciences (Geologische Rundschau), v. 95, p. 529–541.
Ririe, G.T., 1989, Evaporites and strata-bound tungsten mineralization: Geology, v. 17, p. 139–143.
Risse, A., Trumbull, R.B., Coira, B., Kay, S.M., and van den Bogaard, P., 2008, $^{40}Ar/^{39}Ar$ geochronology of mafic volcanism in the back-arc region of the

southern Puna plateau, Argentina: Journal of South American Earth Sciences, v. 26, p. 1–15.
Robinson, P.T., Elders, W.A., and Muffler, L.J.P., 1976, Quaternary volcanism in the Salton Sea geothermal field, Imperial Valley: Geological Society of America Bulletin, v. 87, p. 347–360. doi: 10.1130/0016-7606(1976)87<347:QVITSS>2.0.CO;2
Salisbury, M.J., Jicha, B.R., de Silva, S.L., Singer, B.S., Jiméez, N.C., and Ort, M.H., 2011, $^{40}Ar/^{39}Ar$ chronostratigraphy of Altiplano-Puna volcanic complex ignimbrites reveals the development of a major magmatic province: Geological Society of America Bulletin, v. 123, p. 821–840.
Sarna-Wojcicki, A.M., Pringle, M.S., and Wijbrans, J., 2000, New $^{40}Ar/^{39}Ar$ age of the Bishop tuff from multiple sites and sediment rate calibration for the Matuyama-Brunhes boundary: Journal of Geophysical Research, v. 105, p. 21,431–21,443.
Siebel, W., Schnurr, W.B.W., Hahne, K., Kraemer, B., Trumbull, R.B., van den Bogaard, P., and Emmermann, R., 2001, Geochemistry and isotope systematics of small- to medium-volume Neogene-Quaternary ignimbrites in the southern central Andes: Evidence for derivation from andesitic magma sources: Chemical Geology, v. 171, p. 213–237.
Smith, G.I., 1976, Origin of lithium and other components in the Searles Lake evaporites: U.S. Geological Survey Professional Paper 1005, p. 92–103.
——2009, Late Cenozoic geology and lacustrine history of Searles Valley, Inyo and San Bernardino Counties, California: U.S. Geological Survey Professional Paper 1727, 115 p.
Sparks, R.S.J., Fracnis, P.W., Hamer, R.D., Pankhurst, R.J., O'Callaghan, L.O., Thorpe, R.S., and Page, R., 1985, Ignimbrites of the Cerro Galan caldera, NW Argentina: Journal of Volcanology and Geothermal Research, v. 24, p. 205–248.
Strecker, M.R., Alonso, R.N., Bookhagen, B., Carrapa, B., Hilley, G.E., Sobel, E.R., and Trauth, M.H., 2007, Tectonics and climate of the southern central Andes: Annual Review of Earth and Planetary Sciences, v. 35, p. 747–787.
Toledo, A.O., Alonso, R.N., V. Ruiz, T., and Quiroga, A.G., 2009, Evapofacies Halítica en el Salar del Rincón, Departamento Los Andes, Salta: Revista de la Asociación Geológica Argentina, v. 64, p. 493–500.
Trumbull, R.B., Riller, U., Oncken, O., Scheuber, E., Munier, K., and Hongn, F., 2006, The time-space distribution of Cenozoic volcanism in the south-central Andes: A new data compilation and some tectonic implications, *in* Oncken, O., Chong, G., Franz, G., Giese, P., Götze, H-J., Ramos, V.A., Strecker, M.R., Wigger, P., eds., The Andes—active subduction orogeny: Springer, Berlin, Frontiers in Earth Sciences, v. 1, p. 29–43.
Valero-Garcés, B.L., Grosjean, M., Messerli, B., Schwalb, A., and Kelts, K., 2000, Later Quaternary lacustrine deposition in the Chilean altiplano (18°–28°S): AAPG Studies in Geology, v. 46, p. 625–636.
Vandervoort, D.S., Jordan, T.E., Zeitler, P.K., and Alonso, R.N., 1995, Chronology of internal drainage development and uplift, southern Puna plateau, Argentine central Andes: Geology, v. 23, p. 145–148.
Vinante, D., and Alonso, R.N., 2006, Evapofacies del Salar Hombre Muerto, Puna Argentina: Distribucion y Genesis: Revista de la Asociación Geológica Argentina, v. 61, p. 286–297.
Whelan, J.A., 1969, Subsurface brines and soluble salts of subsurface sediments, Sevier Lake, Millard County, Utah: Utah Geological and Mineral Survey Special Studies 30, 13 p.
White, J.D.L., 1996, Pre-emergent construction of a lacustrine basaltic volcano, Pahvant Butte, Utah (USA): Bulletin of Volcanology, v. 58, p. 249–262.
Winker, C.D., and Kidwell, S.M., 1986, Paleocurrents of the Pliocene Colorado delta plain, Fish bCreek-Vallecito Basin, southern California: Implications for paleogeography of the early northern Gulf of California: Geology, v. 14, p. 788–791.
Woodruff, W.H., Jr., Horton, B.K., Kapp, P., and Stockli, D.F., 2013, Late Cenozoic evolution of the Lunggar extensional basin, Tibet: Implications for basin growth and exhumation in hinterland plateaus: Geological Society of America Bulletin, v. 125, p. 343–358. doi: 10.1130/B30664.1.
Yaksic, A., and Tilton, J., 2009, Using the cumulative availability curve to assess the threat of mineral depletion: The case of lithium: Resources Policy, v. 34, p. 185–194.
Yin, A., Dang, Y.Q., Zhang, M., Chen, X.H., and McRivette, M.W., 2008, Cenozoic tectonic evolution of the Qaidam basin and its surrounding regions (Part 3): Structural geology, sedimentation, and regional tectonic reconstruction: Geological Society of America Bulletin, v. 120, p. 847–876.
Yu, G., Harrison, S.P., and Xue, B., 2001, Lake status records from China: Data Base Documentation: Max Planck Institute for Biogeochemistry (MPI-BGC), MPI-BGC Technical Report 4, 243 p.
Yuan, X., Sobolev, S., and Kind, R., 2002, Moho topography in the central Andes and its geodynamic implications: Earth and Planetary Science Letters, v. 199, p. 389–402.
Zampirro, D., 2004, Hydrogeology of Clayton Valley brine deposits, Esmeralda County, Nevada: Nevada Bureau of Mines and Geology Special Publication 33, p. 271–280.
Zheng, M., 1997, An introduction to saline lakes on the Qinghai-Tibet plateau: Kluwer Academic Publisher, v. 76.
Zheng, M., and Liu, X., 2009.Hydrochemistry of Salt Lakes of the Qinghai-Tibet plateau, China: Aquatic Geochemistry, v. 15, p. 293–320.
Zimmerman, U., Niemeyer, H., and Meffre, S., 2010, Revealing the continental margin of Gondwana: The Ordovician arc of the Cordón de Lila (northern Chile): International Journal of Earth Science (Geologische Rundschau), v. 99, Supplement 1, p. S39–S56.

Table S1. Geochemical Data for Hot Springs, Thermal Water, and Associated Surface Water in Some Li-Rich Brine-Bearing Basins[1]

| Sample no. | Sample date | Sample notes | Sample type | Lat (N) | Long (E) | Elev (m) | $\delta^2H$ | $\delta^{18}O$ | $^{87}Sr/^{86}Sr$ | se | Li mg/L | Na mg/L | K mg/L | Rb µg/L | Cs µg/L | Mg mg/L | Ca mg/L | Sr µg/L | Ba µg/L | As µg/L | U µg/L |
|---|---|---|---|---|---|---|---|---|---|---|---|---|---|---|---|---|---|---|---|---|---|
| Puna Plateau and plateau margin, northwestern Argentina | | | | | | | | | | | | | | | | | | | | | |
| TUC-870 | 27-Mar-07 | Draining metamorphic | River | –27.0915 | –65.5540 | 412 | –28 | –5.9 | 0.72031 | 0.00004 | 0.003 | 3 | 1.8 | 1.2 | <0.03 | 1.1 | 9 | 19 | 18 | 0.25 | 0.03 |
| TUC-872 | 27-Mar-07 | Draining metamoprhic | River | –27.0834 | –65.6655 | 747 | –28 | –5.8 | 0.71802 | 0.00003 | 0.003 | 6 | 2.8 | 1.1 | <0.03 | 2.1 | 11 | 39 | 13 | 0.74 | 0.13 |
| SAL-962 | 3-Apr-07 | Angastaco basin | River | –25.7011 | –66.0295 | 1,772 | –36 | –6.0 | 0.71705 | 0.00001 | 0.497 | 132 | 7.9 | 14 | 1.2 | 9.5 | 37 | 488 | 110 | 21 | 5.3 |
| PUN-1053 | 16-Apr-07 | Rio Aguas Calientes | River | –25.8258 | –66.9247 | 4,461 | –50 | –7.0 | 0.71763 | 0.00002 | 3.25 | 246 | 11 | 164 | 1207 | 6.0 | 32 | 349 | 8 | 799 | 2.7 |
| PUN-1054 | 16-Apr-07 | Hillslope hotspring | Hotspring | –25.8258 | –66.9247 | 4,468 | –50 | –6.5 | 0.71584 | 0.00002 | 5.53 | 389 | 10 | 174 | 1842 | 3.1 | 22 | 315 | 25 | 1806 | 1.5 |
| CAT-1004 | 7-Apr-07 | Termas de Fiambala | Spring (warm) | –27.7430 | –67.5514 | 1,906 | –40 | –6.7 | 0.73561 | 0.00002 | 0.205 | 130 | 3.1 | 38 | 4.6 | 0.63 | 15 | 157 | 53 | 0.19 | 0.05 |
| PUN-1010 | 9-Apr-07 | Salar Carachi Pampa | Lake/ playa | –26.5127 | –67.4092 | 3,014 | 22 | 10.0 | 0.71791 | 0.00001 | 6.48 | >2000 | 201 | 705 | 168 | 86 | 708 | 8018 | 115 | 33 | 8.0 |
| CAT-1014 | 10-Apr-07 | Termas Villavil | Spring (warm) | –27.1123 | –66.8227 | 2,113 | –30 | –4.7 | 0.70959 | 0.00018 | 0.020 | 87 | 1.2 | 1.5 | 0.18 | 0.08 | 7 | 6 | 3 | 4.9 | 0.25 |
| PUN-1051 | 15-Apr-07 | Laguna Grande | Lake/ playa | –26.2379 | –67.0503 | 4,250 | –52 | –6.8 | 0.71897 | 0.00002 | 0.927 | 185 | 13 | 89 | 121 | 6.8 | 45 | 393 | 98 | 140 | 14 |
| Bear River Drainage and Crystal Hot Spring, Great Salt Lake Basin, Utah, USA | | | | | | | | | | | | | | | | | | | | | |
| BR-2 | Nov-12 | Bear River-upstream | River | 41.6384 | –112.1180 | 1,292 | | | 0.71400 | 0.00001 | 0.049 | 57 | 8.2 | 15 | 0.29 | 35 | 59 | 383 | 77 | 2.3 | 1.5 |
| BR-5 | Nov-12 | Bear River-upstream | River | 41.6384 | –112.1185 | 1,292 | | | 0.71408 | 0.00001 | 0.049 | 55 | 8.3 | 16 | 0.33 | 34 | 59 | 383 | 76 | 2.5 | 1.3 |
| BR-3 | Nov-12 | Salt Creek | Creek | 41.6345 | –112.0884 | 1,298 | | | 0.72330 | 0.00002 | 2.37 | 5,249 | 365 | 675 | 63 | 87 | 337 | 13,016 | 233 | 13 | 1.6 |
| BR-4A | Nov-12 | Crystal Hot Spring | Hotspring | 41.6593 | –112.0874 | 1,306 | | | 0.72349 | 0.00002 | 6.65 | 14,863 | 1,012 | 1,899 | 176 | 186 | 806 | 35,499 | 386 | 16 | 0.37 |
| BR-4B | Nov-12 | Crystal Hot Spring | Cold spring | 41.6593 | –112.0874 | 1,306 | | | 0.72297 | 0.00002 | 1.75 | 3,896 | 268 | 501 | 45 | 79 | 279 | 10,063 | 202 | 15 | 3.0 |
| BR-1 | Nov-12 | Bear River-downstream | River | 41.5446 | –112.1080 | 1,289 | | | 0.71623 | 0.00001 | 0.077 | 127 | 11 | 23 | 0.92 | 35 | 62 | 493 | 79 | 2.6 | 1.4 |
| Hot Springs and cold groundwater from the region near Clayton Valley, NV | | | | | | | | | | | | | | | | | | | | | |
| Silver Peak tap | 26-May-11 | 454 Rocky Way | Tap | 37.7568 | –117.6371 | 1,334 | –113 | –14.8 | 0.71019 | 0.00001 | 0.05 | 90 | 3.9 | 4.7 | 0.02 | 24 | 101 | 1,464 | 130 | 1.1 | 12 |
| NHW | 22-May-11 | North Hot Well | Well | 37.7739 | –117.6322 | 1,300 | –117 | –13.1 | 0.71003 | 0.00002 | 39.7 | 10,418 | 899 | 4,060 | 289 | 69 | 641 | 34,643 | 597 | 6.6 | 1.0 |
| CV-24W | 25-May-11 | Groundwater | Well | 37.7146 | –117.5903 | 1,304 | | | 0.70980 | 0.00001 | 6.7 | 1,544 | 288 | 219 | 1.247 | 6 | 37 | 4,789 | 279 | 41 | 0.45 |
| CV-29W | 26-May-11 | Paymaster Hot Well | Well | 37.8314 | –117.4811 | 1,321 | –120 | –14.0 | 0.71175 | 0.00002 | 31.9 | 8,974 | 787 | 3,743 | 293 | 41 | 180 | 8,872 | 177 | 1.1 | 0.05 |
| CV-30W | 26-May-11 | Paymaster Well | Well | 37.8573 | –117.4762 | 1,420 | –124 | –15.6 | 0.71568 | 0.00002 | 0.08 | 87 | 5.9 | 11 | <0.007 | 25 | 52 | 759 | 75 | 0.05 | 0.43 |
| CV-2W | 14-May-12 | Alkali Hot Springs | Hotspring | 37.8246 | –117.3376 | 1,532 | | | 0.71173 | 0.00001 | 1.7 | 314 | 22 | 124 | 83 | 3.7 | 42 | 1,381 | 33 | 5.8 | 0.02 |
| CV-5aW | 13-May-12 | "The Hot Box" | Hotspring | 37.8601 | –117.9840 | 1,448 | | | 0.71250 | 0.00003 | 0.7 | 288 | 28 | 93 | 6 | 0.12 | 4 | 24 | 11 | 54 | 2.9 |
| CV-15W | 13-May-12 | Old Borax Works | Hotspring | 37.9095 | –117.9552 | 1,436 | | | 0.71147 | 0.00001 | 5.3 | 1,382 | 151 | 962 | 320 | 7.4 | 120 | 3,127 | 144 | 711 | 0.08 |
| CV-29W | 15-May-12 | Paymaster Hot Well | Well | 37.8314 | –117.4811 | 1,321 | | | 0.71169 | 0.00001 | 28.2 | 8,974 | 755 | 3,470 | 236 | 35 | 113 | 8,451 | 382 | 0.41 | 0.03 |
| NHW | 16-May-12 | North Hot Well | Well | 37.7739 | –117.6322 | 1,300 | | | 0.71004 | 0.00001 | 34.4 | 10,418 | 852 | 4,075 | 313 | 60 | 656 | 31,719 | 523 | 4.4 | 1.4 |

[1] Elemental data measured by ICP-MS, Sr isotope ratios by MC-ICP-MS, and H and O isotope ratios cavity ring-down spectroscopy